

1 **Trends in secondary inorganic aerosol pollution in China and its responses to**  
2 **emission controls of precursors in wintertime**

3 Fanlei Meng<sup>1#</sup>, Yibo Zhang<sup>2#</sup>, Jiahui Kang<sup>1</sup>, Mathew R. Heal<sup>3</sup>, Stefan Reis<sup>4,3,5</sup>, Mengru  
4 Wang<sup>6</sup>, Lei Liu<sup>7</sup>, Kai Wang<sup>1</sup>, Shaocai Yu<sup>2\*</sup>, Pengfei Li<sup>8</sup>, Jing Wei<sup>9</sup>, Yong Hou<sup>1</sup>, Ying  
5 Zhang<sup>1</sup>, Xuejun Liu<sup>1</sup>, Zhenling Cui<sup>1</sup>, Wen Xu<sup>1\*</sup>, Fusuo Zhang<sup>1</sup>

6  
7 <sup>1</sup>College of Resource and Environmental Sciences; National Academy of Agriculture  
8 Green Development; Key Laboratory of Plant-Soil Interactions of MOE, Beijing Key  
9 Laboratory of Cropland Pollution Control and Remediation, China Agricultural  
10 University, Beijing 100193, China.

11 <sup>2</sup>Research Center for Air Pollution and Health, Key Laboratory of Environmental  
12 Remediation and Ecological Health, Ministry of Education, College of Environment  
13 and Resource Sciences, Zhejiang University, Hangzhou, Zhejiang 310058, P.R. China

14 <sup>3</sup>School of Chemistry, The University of Edinburgh, David Brewster Road, Edinburgh  
15 EH9 3FJ, United Kingdom

16 <sup>4</sup>UK Centre for Ecology & Hydrology, Penicuik, EH26 0QB, United Kingdom.

17 <sup>5</sup>University of Exeter Medical School, Knowledge Spa, Truro, TR1 3HD United  
18 Kingdom.

19 <sup>6</sup>Water Systems and Global Change Group, Wageningen University & Research, P.O.  
20 Box 47, 6700 AA Wageningen, The Netherlands

21 <sup>7</sup>College of Earth and Environmental Sciences, Lanzhou University, Lanzhou 730000,  
22 China

23 <sup>8</sup>College of Science and Technology, Hebei Agricultural University, Baoding, Hebei  
24 071000, China

25 <sup>9</sup>Department of Chemical and Biochemical Engineering, Iowa Technology Institute,  
26 The University of Iowa, Iowa City, IA, USA

27  
28 \*Corresponding authors

29 E-mail addresses: W. Xu ([wenxu@cau.edu.cn](mailto:wenxu@cau.edu.cn)); S C. Yu ([shaocaiyu@zju.edu.cn](mailto:shaocaiyu@zju.edu.cn))

30 <sup>#</sup> Contributed equally to this work.

33 **ABSTRACT:** The Chinese government recently proposed ammonia (NH<sub>3</sub>) emissions  
34 reductions (but without a specific national target) as a strategic option to mitigate PM<sub>2.5</sub>  
35 pollution. We combined a meta-analysis of nationwide measurements and air quality  
36 modelling to identify efficiency gains by striking a balance between controlling NH<sub>3</sub>  
37 and acid gas (SO<sub>2</sub> and NO<sub>x</sub>) emissions. We found that PM<sub>2.5</sub> concentrations decreased  
38 from 2000 to 2019, but annual mean PM<sub>2.5</sub> concentrations still exceeded 35  $\mu\text{g m}^{-3}$  at  
39 74% of 1498 monitoring sites in 2015-2019. Secondary inorganic aerosols (SIA) were  
40 the dominant contributor to ambient PM<sub>2.5</sub> concentrations. The concentration of PM<sub>2.5</sub>  
41 and its components were significantly higher ([16%-195%](#)) on hazy days than on non-  
42 hazy days. Compared with [mean values of](#) other components, this difference was more  
43 significant [for the](#) secondary inorganic ions SO<sub>4</sub><sup>2-</sup>, NO<sub>3</sub><sup>-</sup>, and NH<sub>4</sub><sup>+</sup> ([average increase](#)  
44 [98%](#)). While sulfate concentrations significantly decreased over the time period, no  
45 significant change was observed for nitrate and ammonium concentrations. Model  
46 simulations indicate that the effectiveness of a 50% NH<sub>3</sub> emission reduction for  
47 controlling SIA concentrations decreased from 2010 to 2017 in four megacity clusters  
48 of eastern China, simulated for the month of January under fixed meteorological  
49 conditions (2010). Although the effectiveness further declined in 2020 for simulations  
50 including the natural experiment of substantial reductions in acid gas emissions during  
51 the CoVID-19 pandemic, the resulting reductions in SIA concentrations were on  
52 average 20.8% lower than that in 2017. In addition, the reduction of SIA concentrations  
53 in 2017 was greater for 50% acid gas reductions than for the 50% NH<sub>3</sub> emissions  
54 reduction. Our findings indicate that persistent secondary inorganic aerosol pollution in  
55 China is limited by acid gases emissions, while an additional control on NH<sub>3</sub> emissions  
56 would become more important as reductions of SO<sub>2</sub> and NO<sub>x</sub> emissions progress.

57  
58 **Keywords:** Air pollution, Particulate matter, Second inorganic aerosols, Anthropogenic  
59 emission, Ammonia.

60  
61 **1. Introduction**

62 Over the past two decades, China has experienced severe PM<sub>2.5</sub> (particulate matter  
63 with aerodynamic diameter  $\leq 2.5 \mu\text{m}$ ) pollution (Huang et al., 2014; Wang et al., 2016),  
64 leading to adverse impacts on human health (Liang et al., 2020) and the environment  
65 (Yue et al., 2020). In 2019, elevated PM<sub>2.5</sub> concentrations accounted for 46% of polluted  
66 days in China and PM<sub>2.5</sub> was officially identified as a key year-round air pollutant  
67 (MEEP, 2019). Mitigation of PM<sub>2.5</sub> pollution is therefore the most pressing current  
68 challenge to improve China's air quality.

69 The Chinese government has put a major focus on particulate air pollution control  
70 through a series of policies, regulations, and laws to prevent and control severe air  
71 pollution. Before 2010, the Chinese government mainly focused on controlling SO<sub>2</sub>  
72 emissions via improvement of energy efficiency, with less attention paid to NO<sub>x</sub>  
73 abatement (CSC, 2007, 2011, 2016). For example, the 11<sup>th</sup> Five-Year Plan (FYP) (2006-  
74 2010) set a binding goal of a 10% reduction for SO<sub>2</sub> emission (CSC, 2007). The 12<sup>th</sup>  
75 FYP (2011-2015) added NO<sub>x</sub> regulation and required 8% and 10% reductions for SO<sub>2</sub>  
76 and NO<sub>x</sub> emissions, respectively (CSC, 2011). This was followed by further reductions  
77 in SO<sub>2</sub> and NO<sub>x</sub> emissions of 15% and 10%, respectively, in the 13<sup>th</sup> FYP (2016-2020)  
78 (CSC, 2016). In response to the severe haze events of 2013, the Chinese State Council  
79 promulgated the toughest-ever 'Atmospheric Pollution Prevention and Control Action  
80 Plan' in September 2013, aiming to reduce ambient PM<sub>2.5</sub> concentrations by 15-20% in  
81 2017 relative to 2013 levels in metropolitan regions (CSC, 2013). As a result of the

82 implementation of stringent control measures, emissions reductions markedly  
83 accelerated from 2013-2017, with decreases of 59% for SO<sub>2</sub>, 21% for NO<sub>x</sub>, and 33%  
84 for primary PM<sub>2.5</sub> (Zheng et al., 2018). Consequently, significant reductions in annual  
85 mean PM<sub>2.5</sub> concentrations were observed nationwide (Zhang et al., 2019; Yue et al.,  
86 2020), in the range 28-40% in the metropolitan regions (CSC, 2018a). To continue its  
87 efforts in tackling air pollution, China promulgated the Three-Year Action Plan (TYAP)  
88 in 2018 for Winning the Blue-Sky Defense Battle (CSC, 2018b), which required a  
89 further 15% reduction in NO<sub>x</sub> emissions by 2020 compared to 2018 levels.

90 Despite a substantial reduction in PM<sub>2.5</sub> concentrations in China, the proportion of  
91 secondary aerosols during severe haze periods is increasing (An et al., 2019), and can  
92 comprise up to 70% of PM<sub>2.5</sub> concentrations (Huang et al., 2014). Secondary inorganic  
93 aerosols (SIA, the sum of sulfate (SO<sub>4</sub><sup>2-</sup>), nitrate (NO<sub>3</sub><sup>-</sup>), and ammonium (NH<sub>4</sub><sup>+</sup>)) were  
94 found to be of equal importance to secondary organic aerosols, with 40-50%  
95 contributions to PM<sub>2.5</sub> in eastern China (Huang et al., 2014; Yang et al., 2011). The acid  
96 gases (i.e., NO<sub>x</sub>, SO<sub>2</sub>), together with NH<sub>3</sub>, are crucial precursors of SIA via chemical  
97 reactions that form particulate ammonium sulfate, ammonium bisulfate, and  
98 ammonium nitrate (Ianniello et al., 2010). In addition to the adverse impacts on human  
99 health via fine particulate matter formation (Liang et al., 2020; Kuerban et al., 2020),  
100 large amounts of NH<sub>3</sub> and its aerosol-phase products also lead to nitrogen deposition  
101 and consequently to environmental degradation (Ortiz-Montalvo et al., 2014; Zhan et  
102 al., 2021).

103 Following the successful controls on NO<sub>x</sub> and SO<sub>2</sub> emissions, attention is turning  
104 to NH<sub>3</sub> emissions as a possible means of further PM<sub>2.5</sub> control (Bai et al., 2019; Kang  
105 et al., 2016), particularly as emissions of NH<sub>3</sub> increased between the 1980s and 2010s.  
106 Some studies have found that NH<sub>3</sub> limited the formation of SIA in winter in the eastern

107 United States (Pinder et al., 2007) and Europe (Megaritis et al., 2013). Controls on NH<sub>3</sub>  
108 emissions have been proposed in the TYAP, although mandatory measures and binding  
109 targets have not yet been set (CSC, 2018b). Nevertheless, this proposal means that  
110 China will enter a new phase of PM<sub>2.5</sub> mitigation, with attention now given to both acid  
111 gas and NH<sub>3</sub> emissions. However, in the context of effective control of PM<sub>2.5</sub> pollution  
112 via its SIA component, two key questions arise: 1) what are the responses of the  
113 constituents of SIA to implementation of air pollution control policies, and 2) what is  
114 the relative efficiency of NH<sub>3</sub> versus acid gas emission controls to reduce SIA pollution?

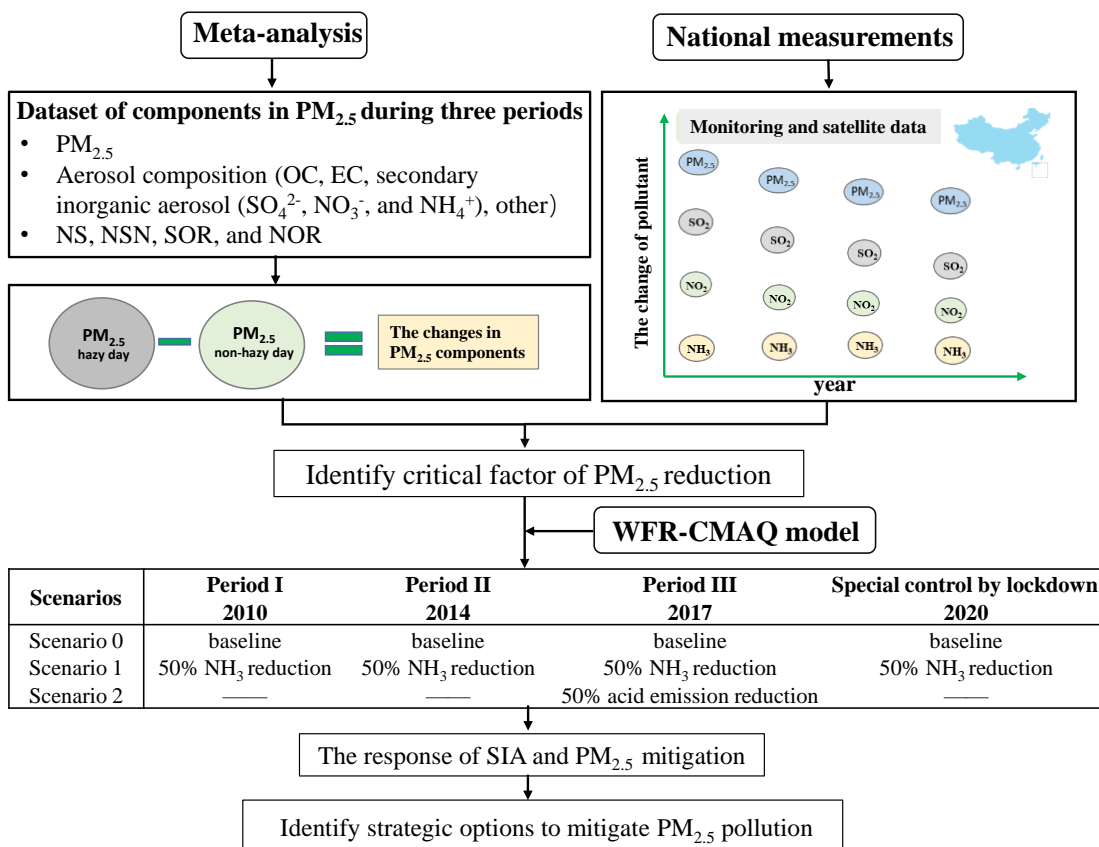
115 To fill this evidence gap and provide useful insights for policy-making to improve  
116 air quality in China, this study adopts an integrated assessment framework. With respect  
117 to the emission control policy summarized above, China's PM<sub>2.5</sub> control can be divided  
118 into three periods: period I (2000–2012), in which PM<sub>2.5</sub> was not the targeted pollutant;  
119 period II (2013–2016), the early stage of targeted PM<sub>2.5</sub> control policy implementation;  
120 and period III (2017–2019), the latter stage with more stringent policies. Therefore, our  
121 research framework consists of two parts: (1) assessment of trends in annual mean  
122 concentrations of PM<sub>2.5</sub>, its chemical components and SIA gaseous precursors from  
123 meta-analyses and observations; (2) quantification of SIA responses to emissions  
124 reductions in NH<sub>3</sub> and acid gases using the Weather Research and Forecasting and  
125 Community Multiscale Air Quality (WRF/CMAQ) models.

126 **2. Materials and methods**

127 **2.1. Research framework**

128 This study developed an integrated assessment framework to analysis the trends of  
129 secondary inorganic aerosol and strategic options to reduce SIA and PM<sub>2.5</sub> pollution in  
130 China (Fig. 1). The difference in PM<sub>2.5</sub> chemical components between hazy and non-  
131 hazy days was first assessed by meta-analysis of published studies. These were

132 interpreted in conjunction with the trends in air concentrations of  $\text{PM}_{2.5}$  and its  
 133 secondary inorganic aerosol precursors ( $\text{SO}_2$ ,  $\text{NO}_2$ , and  $\text{NH}_3$ ) derived from surface  
 134 measurements and satellite observations. The potential of SIA and  $\text{PM}_{2.5}$  concentration  
 135 reductions from precursor emission reductions was then evaluated using the Weather  
 136 Research and Forecasting and Community Multiscale Air Quality (WRF/CMAQ)  
 137 models.



138  
 139 **Fig. 1.** Integrated assessment framework for Chinese  $\text{PM}_{2.5}$  mitigation strategic options.  
 140 OC is organic carbon, EC is elemental carbon,  $\text{NO}_3^-$  is nitrate,  $\text{SO}_4^{2-}$  is sulfate, and  $\text{NH}_4^+$   
 141 is ammonium. NS is the slope of the regression equation between  $[\text{NH}_4^+]$  and  $[\text{SO}_4^{2-}]$ ,  
 142 NSN is the slope of the regression equation between  $[\text{NH}_4^+]$  and  $[\text{SO}_4^{2-} + \text{NO}_3^-]$ , SOR  
 143 is sulfur oxidation ratio, and NOR is nitrogen oxidation ratio. SIA is Secondary  
 144 inorganic aerosols. WRF-CMAQ is Weather Research and Forecasting and Community  
 145 Multiscale Air Quality models.

146 **2.2. Meta-analysis of PM<sub>2.5</sub> and its chemical components**

147 Meta-analyses can be used to quantify the differences in concentrations of PM<sub>2.5</sub> and  
148 its secondary inorganic aerosol components (NH<sub>4</sub><sup>+</sup>, NO<sub>3</sub><sup>-</sup>, and SO<sub>4</sub><sup>2-</sup>) between hazy and  
149 non-hazy days and to identify the major pollutants on non-hazy days (Wang et al.,  
150 2019b); this provides evidence for effective options on control of precursor emissions  
151 (NH<sub>3</sub>, NO<sub>2</sub>, and SO<sub>2</sub>) for reducing occurrences of hazy days. To build a database of  
152 atmospheric concentrations of PM<sub>2.5</sub> and chemical components between hazy and non-  
153 hazy days, we conducted a literature survey using the Web of Science and the China  
154 National Knowledge Infrastructure for papers published between January 2000 and  
155 January 2020. The keywords included: (1) "particulate matter," or "aerosol," or "PM<sub>2.5</sub>"  
156 and (2) "China" or "Chinese". Studies were selected based on the following conditions:  
157 (1) Measurements were taken on both hazy and non-hazy days.  
158 (2) PM<sub>2.5</sub> chemical components were reported.  
159 (3) If hazy days were not defined in the screened articles, the days with PM<sub>2.5</sub>  
160 concentrations > 75  $\mu\text{g m}^{-3}$  (the Chinese Ambient Air Quality Standard Grade II for  
161 PM<sub>2.5</sub> (CSC, 2012)) were treated as hazy days.  
162 (4) If an article reported measurements from different monitoring sites in the same city,  
163 e.g. [Mao et al. \(2018\)](#) and [Xu et al. \(2019\)](#), then each measurement was considered an  
164 independent study.  
165 (5) If there were measurements in the same city for the same year, e.g. [Tao et al. \(2016\)](#)  
166 and [Han et al. \(2017\)](#), then each measurement was treated as an independent study.

167 One hundred articles were selected based on the above conditions with the lists  
168 provided in the Supporting Material dataset. For each selected study, we documented  
169 the study sites, study periods, seasons, aerosol types, and aerosol species mass  
170 concentrations (in  $\mu\text{g m}^{-3}$ ) over the entire study period (2000–2019) (the detailed data

171 are provided in the dataset). In total, the number of sites contributing data to the meta-  
172 analysis was 267 and their locations are shown in Fig. S1. If relevant data were not  
173 directly presented in studies, a GetData Graph Digitizer (Version 2.25,  
174 <http://www.getdatagraph-digitizer.com>) was used to digitize concentrations of PM<sub>2.5</sub>  
175 chemical components from figures. The derivations of other variables such as sulfur  
176 and nitrogen oxidation ratios are described in Supplementary Information Method 1.

177 Effect sizes were developed to normalize the combined studies' outcomes to the  
178 same scale. This was done through the use of log response ratios (lnRR) (Nakagawa et  
179 al., 2012; Ying et al., 2019). The variations in aerosol species were evaluated as follows:

180 
$$\ln RR = \ln \left( \frac{X_p}{X_n} \right) \quad (1)$$

181 where  $X_p$  and  $X_n$  represent the mean values of the studied variables of PM<sub>2.5</sub> components  
182 on hazy and non-hazy days, respectively. The mean response ratio was then estimated  
183 as:

184 
$$RR = \exp \left[ \sum \ln RR(i) \times W(i) / \sum W(i) \right] \quad (2)$$

185 where  $W(i)$  is the weight given to that observation as described below. Finally, variable-  
186 related effects were expressed as percent changes, calculated as  $(RR-1) \times 100\%$ . A 95%  
187 confidence interval not overlapping with zero indicates that the difference is significant.  
188 A positive or negative percentage value indicates an increase or decrease in the response  
189 variables, respectively.

190 We used inverse sampling variances to weight the observed effect size (RR) in the  
191 meta-analysis (Benitez-Lopez et al., 2017). For the measurement sites where standard  
192 deviations (SD) or standard errors (SE) were absent in the original study reports, we  
193 used the "Bracken, 1992" approach to estimate SD (Bracken et al., 1992). The variation-  
194 related chemical composition of PM<sub>2.5</sub> was assessed by random effects in meta-analysis.  
195 Rosenberg's fail safe-numbers ( $N_{fs}$ ) were calculated to assess the robustness of findings

196 on PM<sub>2.5</sub> to publication bias (Ying et al., 2019) (See Table S1). The results (effects)  
197 were considered robust despite the possibility of publication bias if  $N_{fs} > 5 \times n + 10$ ,  
198 where  $n$  indicates the number of sites. The statistical analysis of the concentrations of  
199 PM<sub>2.5</sub> and secondary inorganic ions for three periods used a non-parametric statistical  
200 method since concentrations were not normally distributed based on the Kruskal-Wallis  
201 test (Kruskal and Walls, 1952). For each species, the Kruskal-Wallis one-way analysis  
202 of variance (ANOVA) on ranks among three periods was performed with pairwise  
203 comparison using Dunn's method (Dunn, 1964).

### 204 **2.3. Data collection of air pollutant concentrations**

205 To assess the recent annual trends in China of PM<sub>2.5</sub> and of the SO<sub>2</sub> and NO<sub>2</sub>  
206 gaseous precursors to SIA, real-time monitoring data of these pollutants at 1498  
207 monitoring stations in 367 cities during 2015–2019 were obtained from the China  
208 National Environmental Monitoring Center (CNEMC) (<http://106.37.208.233:20035/>).  
209 This is an open-access archive of air pollutant measurements from all prefecture-level  
210 cities since January 2015. Successful use of data from CNEMC to determine  
211 characteristics of air pollution and related health risks in China has been demonstrated  
212 previously (Liu et al., 2016; Kuerban et al., 2020). The geography stations are shown  
213 in Fig. S1. The annual mean concentrations of the three pollutants at all sites were  
214 calculated from the hourly time-series data according to the method of Kuerban et al.  
215 (2020). Information about sampling instruments, sampling methods, and data quality  
216 controls for PM<sub>2.5</sub>, SO<sub>2</sub>, and NO<sub>2</sub> is provided in Supplementary Method 2. Surface NH<sub>3</sub>  
217 concentrations over China for the 2008–2016 (the currently available) were extracted  
218 from the study of Liu et al. (2019). Further details are in Supplementary Method 2.

### 219 **2.4. WRF/CMAQ model simulations**

220 The Weather Research and Forecasting model (WRFv3.8) and the Models-3

221 community multi-scale air quality (CMAQv5.2) model were used to evaluate the  
222 impacts of emission reductions on SIA and PM<sub>2.5</sub> concentrations over China. The  
223 simulations were conducted at a horizontal resolution of 12 km × 12 km. The simulation  
224 domain covered the whole of China, part of India and east Asia. In the current study,  
225 focus was on the following four regions in China: Beijing-Tianjin-Hebei (BTH),  
226 Yangtze River Delta (YRD), Pearl River Delta (PRD), and Sichuan Basin (SCB). The  
227 model configurations used in this study were the same as those used in Wu et al. (2018a)  
228 and are briefly described here. The WRFv3.8 model was applied to generate  
229 meteorological inputs for the CMAQ model using the National Center for  
230 Environmental Prediction Final Operational Global Analysis (NCEP-FNL) dataset  
231 (Morrison et al., 2009). Default initial and boundary conditions were used in the  
232 simulations. The carbon-bond (CB05) gas-phase chemical mechanism and AERO6  
233 aerosol module were selected in the CMAQ configuration (Guenther et al., 2012).  
234 Anthropogenic emissions for 2010, 2014 and 2017 were obtained from the Multi-  
235 resolution Emission Inventory (<http://meicmodel.org>) with 0.25 ° × 0.25 ° spatial  
236 resolution and aggregated to 12km×12km resolution (Zheng et al., 2018; Li et al., 2017).  
237 Each simulation was spun-up for six days in advance to eliminate the effects of the  
238 initial conditions.

239 The years 2010, 2014 and 2017 were chosen to represent the anthropogenic  
240 emissions associated with the periods I, II, III, respectively. January was selected as the  
241 typical simulation month because wintertime haze pollution frequently occurs in this  
242 month (Wang et al., 2011; Liu et al., 2019b). The sensitivity scenarios of emissions in  
243 January can therefore help to identify the efficient option to control haze pollution.

244 The Chinese government has put a major focus on acid gas emission control  
245 through a series of policies in the past three periods (Fig S2). The ratio decreases of

246 anthropogenic emissions  $\text{SO}_2$  and  $\text{NO}_x$  in January for the years 2010, 2014, 2017 and  
247 2020 are presented in SI [Tables S2 and S3](#), respectively. The emissions from  
248 surrounding countries were obtained from the Emissions Database for Global  
249 Atmospheric Research (EDGAR): HTAPV2. The scenarios and the associated  
250 reductions of  $\text{NH}_3$ ,  $\text{NO}_x$  and  $\text{SO}_2$  for selected four years in three periods can be found  
251 in [Fig. 1](#).

252 The sensitivities of SIA and  $\text{PM}_{2.5}$  to  $\text{NH}_3$  emissions reductions were determined  
253 from the average  $\text{PM}_{2.5}$  concentrations in model simulations without and with an  
254 additional 50%  $\text{NH}_3$  emissions reduction. The choice [of](#) 50% additional  $\text{NH}_3$  emissions  
255 reduction is based on the feasibility and current upper bound of  $\text{NH}_3$  emissions  
256 reduction expected to be [realized](#) in the near future ([Liu et al., 2019a; Table S4](#)). Zhang  
257 et al. (2020) found [that the mitigation potential of  \$\text{NH}\_3\$  emissions from cropland](#)  
258 [production and livestock production in China can reach up to 52% and 58%,](#)  
259 [respectively.](#) To eliminate the influences of varying meteorological conditions, all  
260 simulations were conducted under the fixed meteorological conditions of 2010.

261 During the COVID-19 lockdown in China, emissions of primary pollutants were  
262 subject to unprecedented reductions due to national restrictions on traffic and industry;  
263 in particular, emissions of  $\text{NO}_x$  and  $\text{SO}_2$  reduced by 46% and 24%, respectively,  
264 averaged across all Chinese provinces ([Huang et al., 2021](#)). We therefore also ran  
265 simulations applying the same reductions in  $\text{NO}_x$  and  $\text{SO}_2$  (based on 2017 MEIC) that  
266 were actually observed during the COVID-19 lockdown as a case of special control in  
267 2020.

## 268 [2.5 Model performance](#)

269 The CMAQ model has been extensively used in air quality studies ([Zhang et al.,](#)  
270 [2019; Backes et al., 2016](#)) [and the validity of the chemical regime in the CMAQ model](#)

271 had been confirmed by our previous studies (Zhang et al., 2021a; Wang et al., 2020a,  
272 2021a). In this study, we used surface measurements from previous publications (e.g.,  
273 (Xiao et al., 2020, 2021; Geng et al., 2019; Xue et al., 2019) and satellite observations  
274 to validate the modelling meteorological parameters by WRF model and air  
275 concentrations of PM<sub>2.5</sub> and associated chemical components by CMAQ model. The  
276 meteorological measurements used for validating the WRF model performances were  
277 obtained from the National Climate Data Center (NCDC)  
278 (<ftp://ftp.ncdc.noaa.gov/pub/data/noaa/>). For validation of the CMAQ model, monthly  
279 mean concentrations of PM<sub>2.5</sub> were obtained from Tracking Air pollution in China (TAP,  
280 <http://tapdata.org.cn/>) database. We also collected ground-based observations from  
281 previous publications to validate the modeling concentrations of SO<sub>4</sub><sup>2-</sup>, NO<sub>3</sub><sup>-</sup>, and NH<sub>4</sub><sup>+</sup>.  
282 The detailed information of the monitoring sites are presented in Table S5. Further  
283 information about the modelling is given in Supplementary Method 3 and Figs. S3-S7  
284 and Table S5.

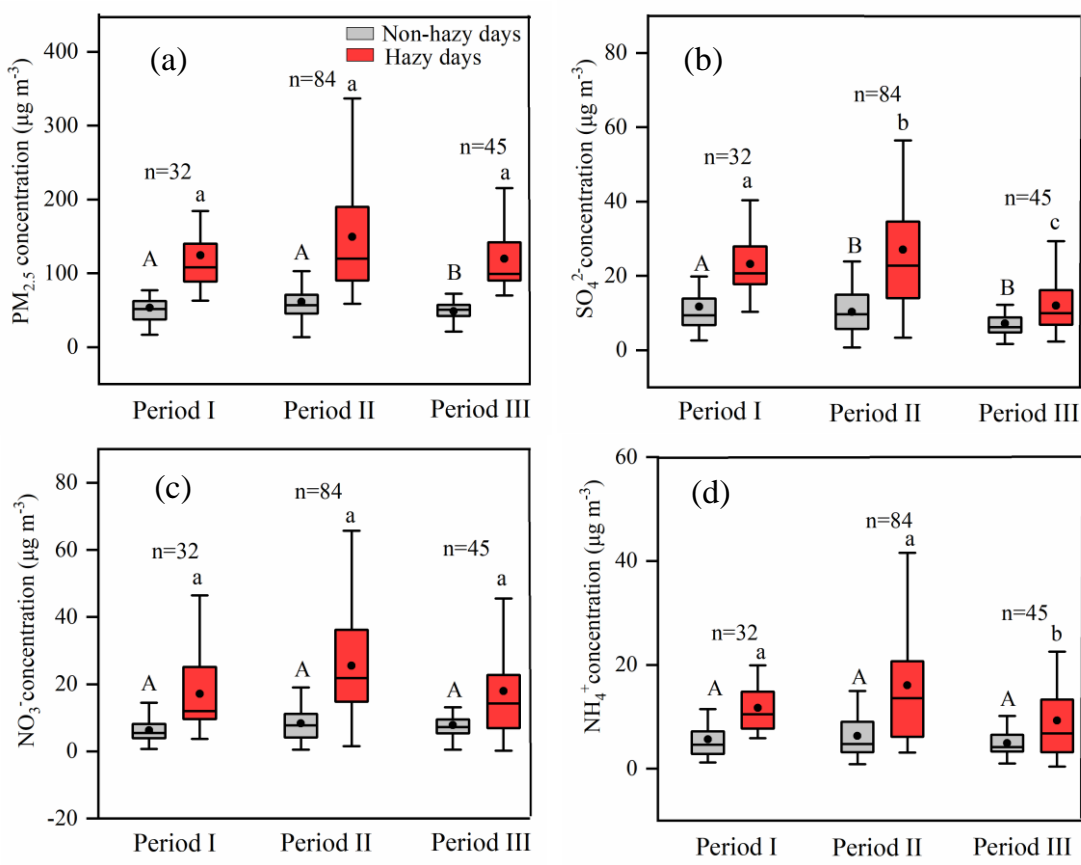
### 285 **3. Results and discussion**

#### 286 **3.1. Characteristics of PM<sub>2.5</sub> and its chemical components from the meta-analysis 287 and from nationwide observations**

288 The meta-analysis based on all published analyses of PM<sub>2.5</sub> and chemical  
289 component measurements during 2000–2019 reveals the changing characteristics of  
290 PM<sub>2.5</sub>. To assess the annual trends in PM<sub>2.5</sub> and its major chemical components, we  
291 made a three-period comparison using the measurements at sites that include both PM<sub>2.5</sub>  
292 and secondary inorganic ions SO<sub>4</sub><sup>2-</sup>, NO<sub>3</sub><sup>-</sup>, and NH<sub>4</sub><sup>+</sup> (Fig. 2). The PM<sub>2.5</sub> concentrations  
293 on both hazy and non-hazy days showed no significant trend from period I and period  
294 II based on Kruskal-Wallis test. However, the observed concentrations of PM<sub>2.5</sub> showed  
295 a downward trend from Period I to Period III on the non-hazy days, decreasing by 8.2%

296 (Fig. 2a), despite no significant decreasing trend on the hazy days (Fig. 2a). In addition,  
 297 the annual mean  $\text{PM}_{2.5}$  concentrations from the nationwide measurements showed  
 298 declining trends during 2015–2019 averaged across all China and for each of the BTH,  
 299 YRD, SCB, and PRD megacity clusters of eastern China (Fig. 3a, d).

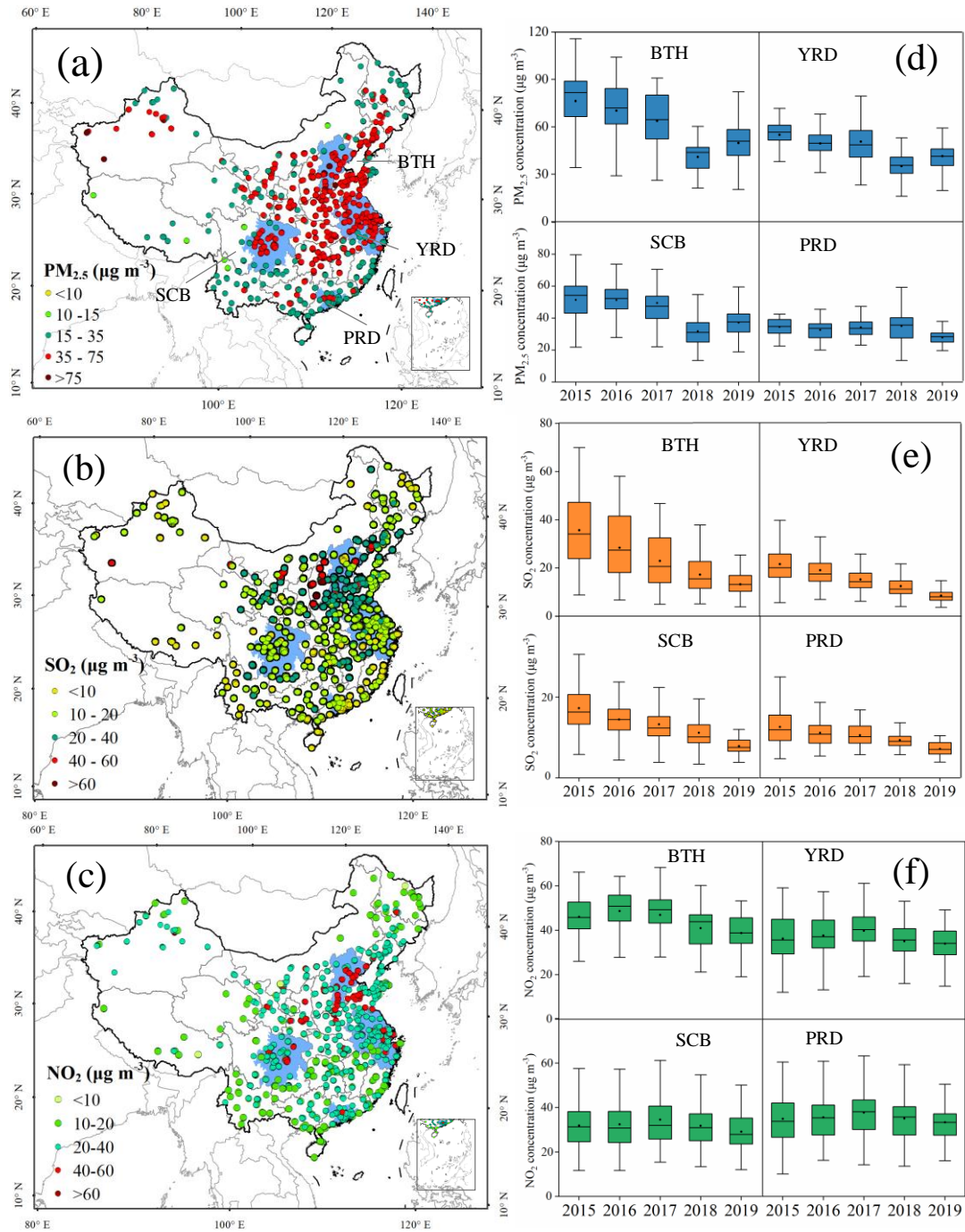
300 These results reflect the effectiveness of the pollution control policies (Fig. S2)  
 301 implemented by the Chinese government at the national scale. Nevertheless,  $\text{PM}_{2.5}$   
 302 remained at relatively high levels. Over 2015–2019, the annual mean  $\text{PM}_{2.5}$   
 303 concentrations at 74% of the 1498 sites (averaging  $51.9 \pm 12.4 \mu\text{g m}^{-3}$ , Fig. 3a) exceeded  
 304 the Chinese Grade-II Standard (GB 3095–2012) of  $35 \mu\text{g m}^{-3}$  (MEPC, 2012), indicating  
 305 that  $\text{PM}_{2.5}$  mitigation is a significant challenge for China.



306  
 307  
 308 **Fig. 2.** Comparisons of observed concentrations of (a)  $\text{PM}_{2.5}$ , (b)  $\text{SO}_4^{2-}$ , (c)  $\text{NO}_3^-$ , and  
 309 (d)  $\text{NH}_4^+$  between non-hazy and hazy days in Period I (2000–2012), Period II (2013–

310 2016), and Period III (2017–2019). Bars with different letters denote significant  
311 differences among the three periods ( $P < 0.05$ ) (upper and lowercase letters for non-  
312 hazy and hazy days, respectively). The upper and lower boundaries of the boxes  
313 represent the 75th and 25th percentiles; the line within the box represents the median  
314 value; the whiskers above and below the boxes represent the 90th and 10th percentiles;  
315 the point within the box represents the mean value. [Comparison of the pollutants among](#)  
316 [the three-periods using Kruskal-Wallis and Dunn's test. The  \$n\$  represents independent](#)  
317 [sites; more detail on this is presented in Section 2.2.](#)

318



319  
320 **Fig. 3.** Left: spatial patterns of annual mean observed concentration of (a) PM<sub>2.5</sub>, (b)  
321 SO<sub>2</sub>, (c) NO<sub>2</sub> at 1498 sites, averaged for 2015–2019. Right: the annual observed  
322 concentrations of (d) PM<sub>2.5</sub>, (e) SO<sub>2</sub>, and (f) NO<sub>2</sub> for 2015-2019 in four megacity  
323 clusters (BTH: Beijing-Tianjin-Hebei, YRD: Yangtze River Delta, SCB: Sichuan Basin,  
324 PRD: Pearl River Delta). The locations of the regions are indicated by the blue shading  
325 on the map. The upper and lower boundaries of the boxes represent the 75th and 25th

326 percentiles; the line within the box represents the median value; the whiskers above and  
327 below the boxes represent the 90th and 10th percentiles; the point within the box  
328 represents the mean value.

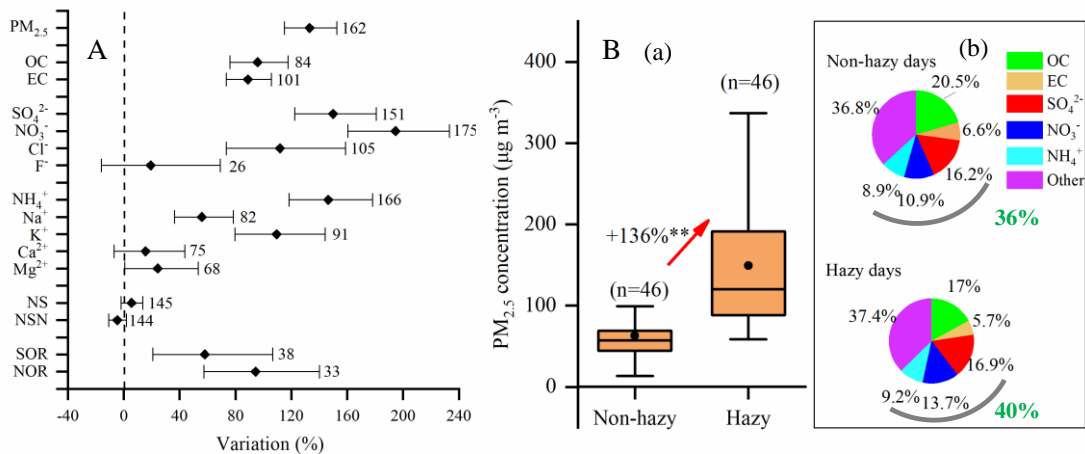
329 To further explore the underlying drivers of PM<sub>2.5</sub> pollution, we analyzed the  
330 characteristics of PM<sub>2.5</sub> chemical components and their temporal changes in China. The  
331 concentrations of PM<sub>2.5</sub> and all its chemical components (except F<sup>-</sup> and Ca<sup>2+</sup>) were  
332 significantly higher on hazy days than on non-hazy days (Fig. 4A). Compared with  
333 other components this difference was more significant for secondary inorganic ions (i.e.,  
334 SO<sub>4</sub><sup>2-</sup>, NO<sub>3</sub><sup>-</sup>, and NH<sub>4</sub><sup>+</sup>). Sulfur oxidation ratio (SOR) and nitrogen oxidation ratio  
335 (NOR) were also 58.0% and 94.4% higher on hazy days than on non-hazy days,  
336 respectively, implying higher oxidations of gaseous species to sulfate- and nitrate-  
337 containing aerosols on the hazy days (Sun et al., 2006; Xu et al., 2017).

338 To provide quantitative information on differences in PM<sub>2.5</sub> and its components  
339 between hazy days and non-hazy days, we made a comparison using 46 groups of data

340 on simultaneous measurements of PM<sub>2.5</sub> and chemical components. The 46 groups refer  
341 to independent analyses from the literature that compare concentrations of PM<sub>2.5</sub> and  
342 major components (SO<sub>4</sub><sup>2-</sup>, NO<sub>3</sub><sup>-</sup>, NH<sub>4</sub><sup>+</sup>, OC, and EC) on hazy and non-hazy days

343 measured across different sets of sites. As shown in Fig.4B\_(a), PM<sub>2.5</sub> concentrations  
344 significantly increased (by 136%) on the hazy days ( $149.2 \pm 81.6 \mu\text{g m}^{-3}$ ) relative to  
345 those on the non-hazy days ( $63.2 \pm 29.8 \mu\text{g m}^{-3}$ ). By contrast, each component's  
346 proportions within PM<sub>2.5</sub> differed slightly, with 36% and 40% contributions by SIA on  
347 non-hazy days and hazy days, respectively (Fig. 4B(b)). This is not surprising because  
348 concentrations of PM<sub>2.5</sub> and SIA both significantly increased on the hazy days ( $60.1 \pm$   
349  $37.4 \mu\text{g m}^{-3}$  for SIA) relative to the non-hazy days ( $22.4 \pm 12.1 \mu\text{g m}^{-3}$  for SIA). Previous  
350 studies have found that increased SIA formation is the major influencing factor for haze

351 pollution in wintertime and summertime (mainly in years since 2013) in major Chinese  
 352 cities in eastern China (Huang et al., 2014; Wang et al., 2019a; Li et al., 2018). Our  
 353 results extend confirmation of the dominant role of SIA to  $\text{PM}_{2.5}$  pollution over a large  
 354 spatial scale in China and to longer temporal scales.

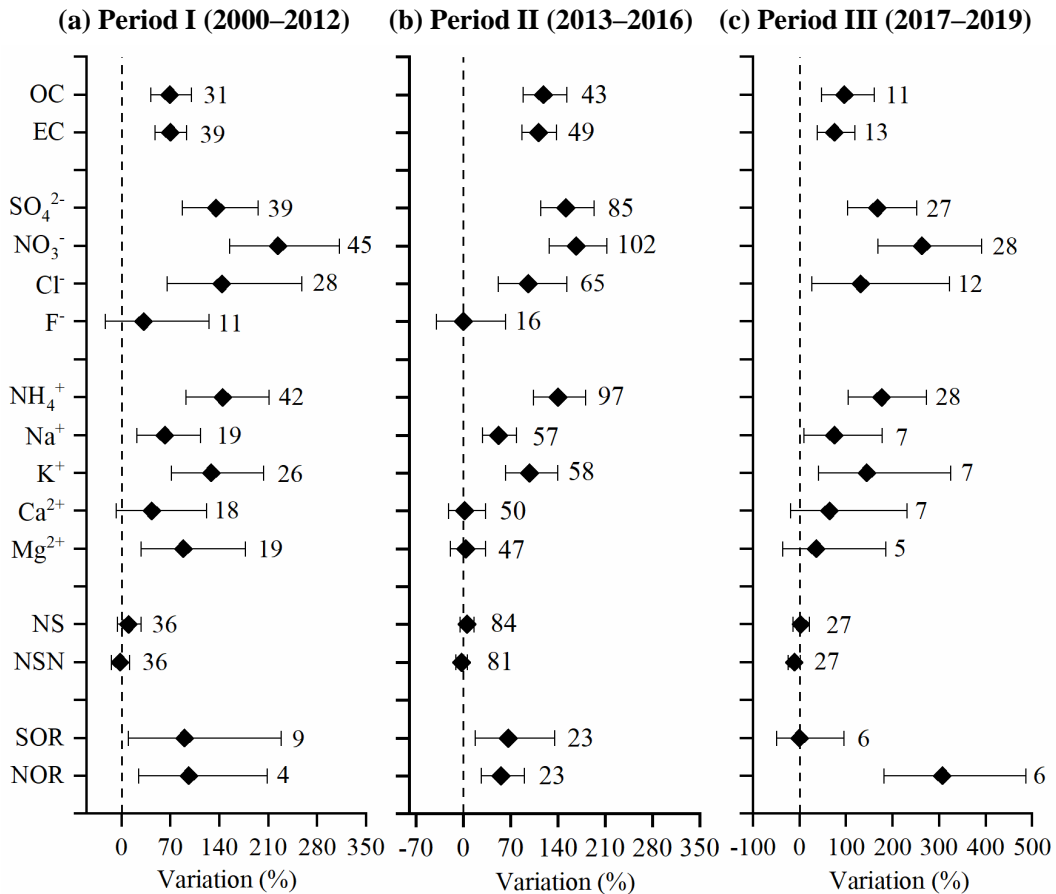


355  
 356 **Fig. 4.** (A) Variations in  $\text{PM}_{2.5}$  concentration, aerosol component concentration, NS,  
 357 NSN, SOR, and NOR from non-hazy to hazy days in China during 2000–2019. (B) (a)  
 358 Summary of differences in  $\text{PM}_{2.5}$  concentration between non-hazy and hazy days in  
 359 China; (b) the average proportions of components of  $\text{PM}_{2.5}$  on non-hazy and hazy days.  
 360 NS is the slope of the regression equation between  $[\text{NH}_4^+]$  and  $[\text{SO}_4^{2-}]$ , NSN is the slope  
 361 of the regression equation between  $[\text{NH}_4^+]$  and  $[\text{SO}_4^{2-} + \text{NO}_3^-]$ , SOR is sulfur oxidation  
 362 ratio, and NOR is nitrogen oxidation ratio. The variations are considered significant if  
 363 the confidence intervals of the effect size do not overlap with zero. \*\* denotes significant  
 364 difference ( $P < 0.01$ ) between hazy days and non-hazy days. The upper and lower  
 365 boundaries of the boxes represent the 75th and 25th percentiles; the line within the box  
 366 represents the median value; the whiskers above and below the boxes represent the 90th  
 367 and 10th percentiles; the point within the box represents the mean value. Values  
 368 adjacent to each confidence interval indicate number of measurement sites. The n  
 369 represents independent sites; more detail on this is presented in Section 2.2.

370 The effect values of SIA on the hazy days were significantly higher than those on  
371 non-hazy days for all three periods (I, II, and III) (Fig. 5), indicating the persistent  
372 prevalence of the SIA pollution problem over the past two decades. Considering  
373 changes in concentrations,  $\text{SO}_4^{2-}$  showed a downward trend from Period I to Period III  
374 on the non-hazy days and hazy day, decreasing by 38.6% and 48.3%, respectively (Fig.  
375 2b). These results reflect the effectiveness of the  $\text{SO}_2$  pollution control policies (Ronald  
376 et al., 2017). In contrast, there were no significant downward trends in concentrations  
377 of  $\text{NO}_3^-$  and  $\text{NH}_4^+$  on either hazy or non-hazy days (Fig. 2c, d), but the mean  $\text{NO}_3^-$   
378 concentration in Period III decreased by 10.5% compared with that in Period II,  
379 especially on hazy days (-16.8%). These results could be partly supported by decreased  
380  $\text{NO}_x$  emissions and tropospheric  $\text{NO}_2$  vertical column densities between 2011 and 2019  
381 in China owing to effective  $\text{NO}_x$  control policies (Zheng et al., 2018; Fan et al., 2021).  
382 The lack of significantly downward trends in  $\text{NH}_4^+$  concentrations may be due to the  
383 fact that the total  $\text{NH}_3$  emissions in China changed little and remained at high levels  
384 between 2000 and 2018, i.e., slightly decreased from 2000 (10.3 Tg) to 2012 (9.3 Tg)  
385 (Kang et al., 2016) and then slightly increased between 2013 and 2018 (Liu et al., 2021).  
386 The similar trends are also found in Quzhou in China, which is a long-term in situ  
387 monitoring site (in Quzhou County, North China Plain, operated by our group) during  
388 the period 2012-2020 from previous publications (Xu et al., 2016; Zhang et al., 2021b,  
389 noted that data during 2017-2020 are unpublished before) (Fig. S8). Zhang et al. (2020)  
390 found that the clean air actions implemented in 2017 effectively reduced wintertime  
391 concentrations of  $\text{PM}_{1}$  (particulate matter with diameter  $\leq 1 \mu\text{m}$ ),  $\text{SO}_4^{2-}$  and  $\text{NH}_4^+$  in  
392 Beijing compared with those in 2007, but had no apparent effect on  $\text{NO}_3^-$ . Our findings  
393 are to some extent supported by the nationwide measurements. Annual mean  $\text{SO}_2$   
394 concentrations displayed a clear decreasing trend with a 53% reduction in 2019 relative

395 to 2015 for the four megacity clusters of eastern China (Fig. 3b, e), whereas there were  
396 only slight reductions in annual mean  $\text{NO}_2$  concentrations (Fig. 3c, f). In contrast,  
397 annual mean  $\text{NH}_3$  concentrations showed an obvious increasing trend in both  
398 northern and southern regions of China, and especially in the BTH region (Fig. S9).

399 Overall, the above analyses indicate that  $\text{SO}_4^{2-}$  concentrations responded  
400 positively to air policy implementations at the national scale, but that reducing  $\text{NO}_3^-$   
401 and  $\text{NH}_4^+$  remains a significant challenge. China has a history of around 10-20 years  
402 for  $\text{SO}_2$  and  $\text{NO}_x$  emission control and has advocated  $\text{NH}_3$  controls despite to date no  
403 mandatory measures and binding targets having been set (Fig. S2). Nevertheless,  $\text{PM}_{2.5}$   
404 pollution, especially SIA such as  $\text{NO}_3^-$  and  $\text{NH}_4^+$ , is currently a serious problem (Fig. 4  
405 and 5a, b). Some studies have reported that  $\text{PM}_{2.5}$  pollution can be effectively reduced  
406 if implementing synchronous  $\text{NH}_3$  and  $\text{NO}_x/\text{SO}_2$  controls (Liu et al., 2019b). Therefore,  
407 based on the above findings, we propose that  $\text{NH}_3$  and  $\text{NO}_x/\text{SO}_2$  emission mitigation  
408 should be simultaneously strengthened to mitigate haze pollution.



409 **Fig. 5.** Variations in PM<sub>2.5</sub> composition, NS, NSN, SOR, and NOR from non-hazy to  
 410 hazy days in (a) Period I (2000–2012), (b) Period II (2013–2016), (c) Period III (2017–  
 411 2019). NS is the slope of the regression equation between [NH<sub>4</sub><sup>+</sup>] and [SO<sub>4</sub><sup>2-</sup>], NSN is  
 412 the slope of the regression equation between [NH<sub>4</sub><sup>+</sup>] and [SO<sub>4</sub><sup>2-</sup> + NO<sub>3</sub><sup>-</sup>], SOR is sulfur  
 413 oxidation ratio, and NOR is nitrogen oxidation ratio. The variations are statistically  
 414 significant if the confidence intervals of the effect size do not overlap with zero. Values  
 415 adjacent to each confidence interval indicate number of measurement sites. The n  
 416 represents independent sites; more detail on this is presented in Section 2.2.  
 417

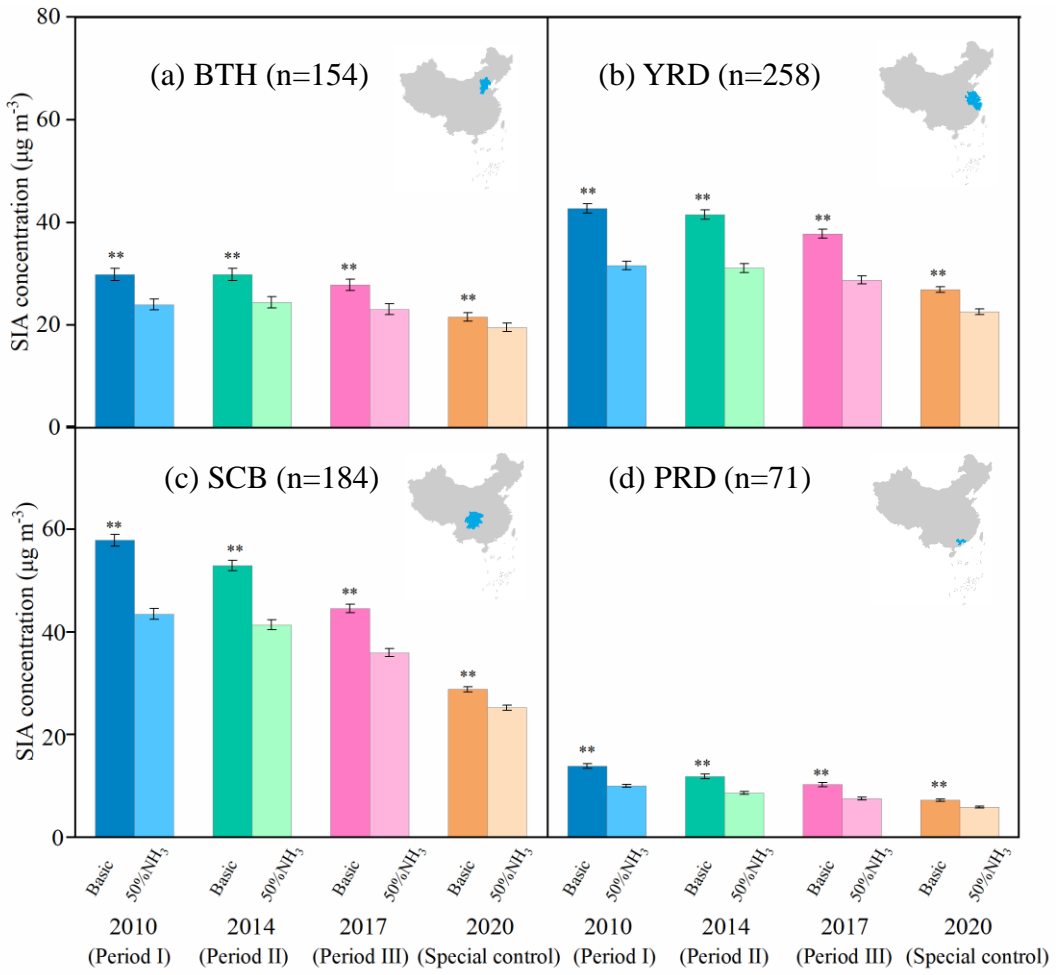
418 **3.2. Sensitivities from model simulations**

419 To further examine the efficiencies of NH<sub>3</sub> and acid gas emission reductions on  
 420 SIA and PM<sub>2.5</sub> mitigation, the decreases of mean SIA and PM<sub>2.5</sub> concentrations with and  
 421 without additional 50% NH<sub>3</sub> reductions were simulated using the WRF/CMAQ model.

422 Fig. 6 and Fig S10 shows that, compared to 2010, SIA and PM<sub>2.5</sub> concentrations in  
423 January in 2017 were significantly decrease in the BTH, YRD, SCB, and PRD megacity  
424 clusters, respectively, in the simulations without additional NH<sub>3</sub> emission reductions.  
425 Across the four megacity clusters, the reduction in SIA and PM<sub>2.5</sub> is largest in the SCB  
426 region from 2010 to 2017 and smallest in the PRD region.

427 When simulating the effects of an additional 50% NH<sub>3</sub> emissions reductions in  
428 January in each of the years 2010, 2014 and 2017, the SIA concentrations in the BTH,  
429 YRD, SCB and PRD megacity clusters decreased by  $25.9 \pm 0.3\%$ ,  $24.4 \pm 0.3\%$ , and  
430  $22.9 \pm 0.3\%$ , respectively (Fig. 6 and Fig. S11). The reductions of PM<sub>2.5</sub> in 2010, 2014  
431 and 2017 were  $9.7 \pm 0.1\%$ ,  $9.0 \pm 0.1\%$ , and  $9.2 \pm 0.2\%$  in the megacity clusters,  
432 respectively. (Figs. S10 and S12). Whilst these results confirm the effectiveness of NH<sub>3</sub>  
433 emission controls, it is important to note that the response of SIA concentrations is less  
434 sensitive to additional NH<sub>3</sub> emission controls along the timeline of the SO<sub>2</sub> and NO<sub>x</sub>  
435 anthropogenic emissions reductions associated with the series of clean air actions  
436 implemented by the Chinese government from 2010 to 2017 (Zheng et al., 2018). Given  
437 the feasibility and current upper bound of NH<sub>3</sub> emission reductions options in the near  
438 future (50%) (Liu et al., 2019b), further abatement of SIA concentrations merely by  
439 reducing NH<sub>3</sub> emissions is limited in China. In other words, the controls on acid gas  
440 emissions should continue to be strengthened beyond their current levels.

441

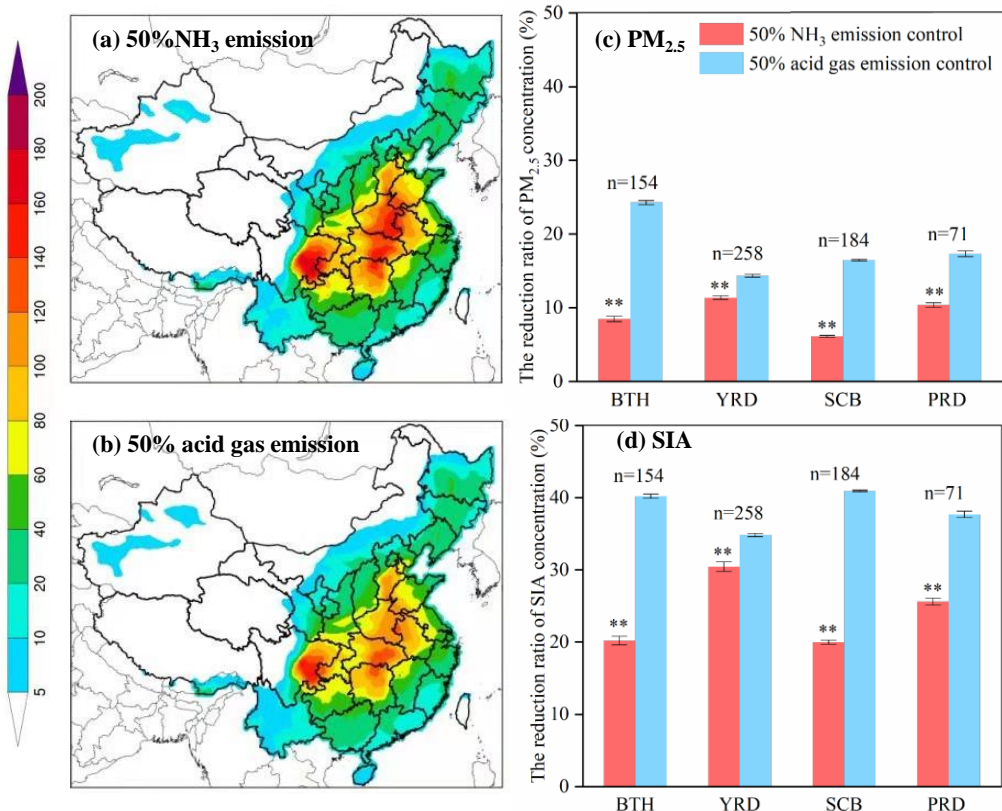


442

443 **Fig. 6.** Simulated SIA concentrations (in  $\mu\text{g m}^{-3}$ ) without (basic) and with 50%  
444 ammonia (NH<sub>3</sub>) emissions reductions in January for the years 2010, 2014, 2017 and  
445 2020 in four megacity clusters (BTH: Beijing-Tianjin-Hebei, YRD: Yangtze River  
446 Delta, SCB: Sichuan Basin, PRD: Pearl River Delta). Inset maps indicate the location  
447 of each region. \*\* denotes significant difference without and with 50% ammonia  
448 emission reductions ( $P < 0.05$ ).  $n$  is the number of calculated samples by grid extraction.  
449 Error bars are standard errors of means. (Period I (2000–2012), Period II (2013–2016),  
450 and Period III (2017–2019); Special control is the restrictions in economic activities  
451 and associated emissions during the COVID-19 lockdown period in 2020.)

452 To further verify the above findings, we used the reductions of emissions of acid  
453 gases (46% and 23% for NO<sub>x</sub> and SO<sub>2</sub>, respectively, in the whole China) during the

454 COVID-lockdown period as a further scenario (Huang et al., 2021). The model  
455 simulations suggest that the effectiveness of reductions in SIA and PM<sub>2.5</sub> concentrations  
456 by a 50% NH<sub>3</sub> emission reduction further declined in 2020 ( $15 \pm 0.2\%$  for SIA, and  
457  $5.1 \pm 0.2\%$  for PM<sub>2.5</sub>), but the resulting concentrations of them were lower ( $20.8 \pm 0.3\%$   
458 for SIA, and  $15.6 \pm 0.3\%$  for PM<sub>2.5</sub>) when compared with that in 2017 under the same  
459 scenario of an additional 50% NH<sub>3</sub> emissions reduction (and constant meteorological  
460 conditions) (Fig. 6), highlighting the importance of concurrently NH<sub>3</sub> mitigation when  
461 acid gas emissions are strengthened. To confirm the importance of acid gas emissions,  
462 another sensitivity simulation was conducted for 2017, in which the acid gas (NO<sub>x</sub> and  
463 SO<sub>2</sub>) emissions were reduced by 50% (Fig. 7). We found that reductions in SIA  
464 concentrations are  $13.4 \pm 0.5\%$  greater for the 50% reductions in SO<sub>2</sub> and NO<sub>x</sub>  
465 emissions than for the 50% reductions in NH<sub>3</sub> emissions. These results indicate that to  
466 substantially reduce SIA pollution it remains imperative to strengthen emission controls  
467 on NO<sub>x</sub> and SO<sub>2</sub> even when a 50% reduction in NH<sub>3</sub> emission is targeted and achieved.



468

469 **Fig. 7.** Left: the spatial distributions of simulated  $\text{PM}_{2.5}$  concentrations (in  $\mu\text{g m}^{-3}$ ) in  
470 January 2017 with (a) 50% reductions in ammonia (NH<sub>3</sub>) emissions and (b) 50%  
471 reductions in acid gas (NO<sub>x</sub> and SO<sub>2</sub>) emissions. Right: the % decreases in  $\text{PM}_{2.5}$  (c)  
472 and SIA (d) concentrations for the simulations with compared to without the NH<sub>3</sub> and  
473 acid gas emissions reductions in four megacity clusters (BTH: Beijing-Tianjin-Hebei,  
474 YRD: Yangtze River Delta, SCB: Sichuan Basin, PRD: Pearl River Delta). \*\* denotes  
475 significant differences without and with 50% ammonia emission reductions ( $P < 0.05$ ).  
476  $n$  is the number of calculated samples by grid extraction. Error bars are standard errors  
477 of means.

478

### 3.3. Uncertainty analysis and limitations

479

Some limitations should be noted in interpreting the results of the present study: this  
480 study examined period-to-period changes in  $\text{PM}_{2.5}$  chemical components based on a  
481 meta-analysis and the efficiencies of NH<sub>3</sub> and acid gas emission reductions on  $\text{PM}_{2.5}$

482 mitigation. Some uncertainties may still exist in meta-analysis of nationwide  
483 measurements owing to differences in monitoring, sample handling and analysis  
484 methods as well as lack of long-term continuous monitoring sites (Fig. 2). For example,  
485 the measurements of PM<sub>2.5</sub> were mainly taken using the TEOM method, which is  
486 associated with under-reading of PM due to some nitrate volatilization at its operational  
487 temperature. To test whether the use of data during 2000–2019 could bias annual trends  
488 of PM<sub>2.5</sub> and chemical components, we summarize measurements of PM<sub>2.5</sub> at a long-  
489 term monitoring site (in Quzhou County, North China Plain, operated by our group)  
490 during the period 2012-2020 from previous publications (Xu et al., 2016; Zhang et al.,  
491 2021, noted that data during 2017-2020 are unpublished before). The PM<sub>2.5</sub> and SO<sub>4</sub><sup>2-</sup>  
492 show the same decreasing trend. The concentration of NO<sub>3</sub><sup>-</sup> and NH<sub>4</sub><sup>+</sup> do not show  
493 significant change (Fig. S8). The results are consistent with the trend for the whole of  
494 China obtained from the meta-analysis.

495 WRF-CMAQ model performance also has some uncertainty. We performed the  
496 validations of WRF and CMAQ models. The simulations of temperature at 2 m above  
497 ground (T2), wind speed (WS), and relative humidity (RH) versus observed values at  
498 400 monitoring sites in China are shown in Fig. S7. The meteorological measurements  
499 were obtained from the National Climate Data Center (NCDC)  
500 (<ftp://ftp.ncdc.noaa.gov/pub/data/noaa/>). The comparisons showed that the model  
501 performed well at predicting meteorological parameters with *R* values of 0.94, 0.64 and  
502 0.82 for T2, WS and RH, respectively. However, the WS was overestimated (22.3%  
503 NMB) in most regions of China, which is also reported in previous studies (Gao et al.,  
504 2016; Chen et al., 2019). This may be related to the underlying surface parameters set  
505 in the WRF model configurations.

506 In addition, the simulations of PM<sub>2.5</sub> and associated chemical components by the

507 CMAQ model have potential biases in the spatial pattern, although the CMAQ model  
508 has been extensively used in air quality studies (Zhang et al., 2019; Backes et al., 2016)  
509 and the validity of the chemical regime in the CMAQ model had been confirmed by  
510 our previous studies (Zhang et al., 2021a; Wang et al., 2020a, 2021a). Since nationwide  
511 measurements of PM<sub>2.5</sub> and associated chemical components are lacking in 2010 in  
512 China, we undertook our own validation of PM<sub>2.5</sub> and its components (such as SO<sub>4</sub><sup>2-</sup>,  
513 NO<sub>3</sub><sup>-</sup>, and NH<sub>4</sub><sup>+</sup>) using a multi-observation dataset that includes those monitoring data  
514 and satellite observations at a regional scale that were available.

515 First, the simulated monthly mean PM<sub>2.5</sub> concentration in January 2010 was  
516 compared with corresponding data obtained from the Tracking Air pollution in China  
517 (TAP, <http://tapdata.org.cn/>) database. The satellite historical PM<sub>2.5</sub> predictions are  
518 reliable (average  $R^2 = 0.80$  and RMSE = 11.26  $\mu\text{g m}^{-3}$ ) in a validation against the in-  
519 situ surface observations on a monthly basis (Wei et al., 2020, 2021). The model well  
520 captured the spatial distributions of PM<sub>2.5</sub> concentrations in our studied regions of BTH,  
521 YRD, PRD, and SCB (Fig. S3a), with correlation coefficient ( $R$ ) between simulated and  
522 satellite observed PM<sub>2.5</sub> concentrations of 0.96, 0.80, 0.60, and 0.85 for BTH, YRD,  
523 PRD, and SCB, respectively.

524 Second, we also collected ground-based observations from previous publications  
525 (Xiao et al., 2020, 2021; Geng et al., 2019; Xue et al., 2019) to validate the modeling  
526 concentrations of SO<sub>4</sub><sup>2-</sup>, NO<sub>3</sub><sup>-</sup>, and NH<sub>4</sub><sup>+</sup>. Detailed information about the monitoring  
527 sites is presented in Table S5. The distributions of the simulated monthly mean  
528 concentrations of SO<sub>4</sub><sup>2-</sup>, NO<sub>3</sub><sup>-</sup>, and NH<sub>4</sub><sup>+</sup> in January 2010 over China is compared with  
529 collected surface measurements are shown in Fig. S4a, b, and c, respectively, with their  
530 linear regression analysis presented in Fig. S4d. The model showed underestimation in  
531 simulating SO<sub>4</sub><sup>2-</sup> and NO<sub>3</sub><sup>-</sup> in the BTH region, which might be caused by the uncertainty

532 in the emission inventory. The lack of heterogeneous pathways for  $\text{SO}_4^{2-}$  formation in  
533 the CMAQ model might also be an important reason for the negative bias between  
534 simulations and measurements (Yu et al., 2005; Cheng et al., 2016). The model  
535 overestimated  $\text{NO}_3^-$  concentration in the SCB region, but can capture the spatial  
536 distribution of  $\text{NO}_3^-$  in other regions. The overestimation of  $\text{NO}_3^-$  has been a common  
537 problem in regional chemical transport models such as CMAQ, GEOS-CHEM and  
538 CAMx (Yu et al., 2005; Fountoukis et al., 2011; Zhang et al., 2012; Wang et al., 2013),  
539 due to the difficulties in correctly capturing the gas and aerosol-phase nitrate  
540 partitioning (Yu et al., 2005). The modeling of  $\text{NH}_4^+$  concentrations show good  
541 agreement with the observed values. Generally, the evaluation results indicate that the  
542 model reasonably predicted concentrations of  $\text{SO}_4^{2-}$ ,  $\text{NO}_3^-$ , and  $\text{NH}_4^+$  in  $\text{PM}_{2.5}$ .

543 Third, we performed a comparison of the time-series of the observed and simulated  
544 hourly  $\text{PM}_{2.5}$  and its precursors ( $\text{SO}_2$  and  $\text{NO}_2$ ) during January 2010. The model well  
545 captures the temporal variations of the  $\text{PM}_{2.5}$  in Beijing, with an NMB value of 0.05  $\text{ug}$   
546  $\text{m}^{-3}$ , NME of 28%, and  $R$  of 0.92 (Fig. 5a). The predicted daily concentrations of  $\text{NO}_2$   
547 and  $\text{SO}_2$  during January 2010 also show good agreement with the ground measurements  
548 in Beijing, with NMB and  $R$  values of 0.12  $\text{ug m}^{-3}$  and 0.89 for  $\text{NO}_2$ , and -0.04, 0.95  
549 for  $\text{SO}_2$ , respectively (Fig. 5b). The variations of daily  $\text{PM}_{2.5}$  concentrations between  
550 simulation and observation at 4 monitoring sites (Shangdianzi, Chengdu, Institute of  
551 Atmospheric Physics, Chinese Academy of Sciences (IAP-CAS), and Tianjin) from 14  
552 to 30 January 2010 also matched well, with NMB values ranging from -0.05 to 0.12  $\text{ug}$   
553  $\text{m}^{-3}$ , and  $R$  values exceeding 0.89 (Fig S5c).

554 We also compared the simulated and observed concentrations of  $\text{PM}_{2.5}$ ,  $\text{NO}_2$ , and  
555  $\text{SO}_2$  in China in pre-COVID period (1–26 January 2020) and during the COVID-  
556 lockdown period (27 January–26 February). As shown in Fig. S6, both the simulations

557 and observations suggested that the PM<sub>2.5</sub> and NO<sub>2</sub> concentrations substantially  
558 decreased during the COVID-lockdown, mainly due to the sharp reduction in vehicle  
559 emissions (Huang et al., 2021; Wang et al., 2021b). For SO<sub>2</sub>, the concentrations  
560 decreased very little and even increased at some monitoring sites. The model  
561 underestimated the concentrations of PM<sub>2.5</sub>, NO<sub>2</sub>, and SO<sub>2</sub>, with NMB values of -21.4%,  
562 -22.1%, and -9.6%, respectively. This phenomenon is reasonable as the simulations for  
563 the two periods in 2020 used the meteorology for 2010 whereas measured changes are  
564 strongly influenced by the actual meteorological conditions.

565 **3.4. Implication and outlook**

566 Improving air quality is a significant challenge for China and the world. A key  
567 target in China is for all cities to attain annual mean PM<sub>2.5</sub> concentrations of 35  $\mu\text{g m}^{-3}$   
568 or below by 2035 (Xing et al., 2021). However, this study has shown that 74% of 1498  
569 nationwide measurement sites have exceeded this limit value in recent years (averaged  
570 across 2015-2019). Our results indicated that acid gas emissions still need to be a focus  
571 of control measures, alongside reductions in NH<sub>3</sub> emissions, in order to reduce SIA (or  
572 PM<sub>2.5</sub>) formation. Model simulations for the month of January underpin the finding that  
573 the relative effectiveness of NH<sub>3</sub> emission control decreased over the period from 2010  
574 to 2017. However, simulating the substantial emission reductions in acid gases due to  
575 the lockdown during the COVID-19 pandemic, with fossil fuel-related emissions  
576 reduced to unprecedented levels, indicated the importance of ammonia emission  
577 abatement for PM<sub>2.5</sub> air quality improvements when SO<sub>2</sub> and NO<sub>x</sub> emissions have  
578 already reached comparatively low levels. Therefore, a strategic and integrated  
579 approach to simultaneously undertaking acid gas emissions and NH<sub>3</sub> mitigation is  
580 essential to substantially reduce PM<sub>2.5</sub> concentrations. However, the mitigation of acid

581 gas and NH<sub>3</sub> emissions pose different challenges due to different sources they originate  
582 from.

583 The implementation of further reduction of acid gas emissions is challenging. The  
584 prevention and control of air pollution in China originally focused on the control of acid  
585 gas emissions ([Fig.S2](#)). The controls have developed from desulfurization and  
586 denitrification technologies in the early stages to advanced end-of-pipe control  
587 technologies. By 2018, over 90% of coal-fired power plants had installed end-of-pipe  
588 control technologies ([CEC, 2020](#)). The potential for further reductions in acid gas  
589 emissions by end-of-pipe technology might therefore be limited. Instead, addressing  
590 total energy consumption and the promotion of a transition to clean energy through a  
591 de-carbonization of energy production is expected to be an inevitable requirement for  
592 further reducing PM<sub>2.5</sub> concentrations ([Xing et al., 2021](#)). In the context of improving  
593 air quality and mitigating climate change, China is adopting a portfolio of low-carbon  
594 policies to meet its Nationally Determined Contribution pledged in the Paris Agreement.  
595 Studies show that if energy structure adjusts and energy conservation measures are  
596 implemented, SO<sub>2</sub> and NO<sub>x</sub> will be further reduced by 34% and 25% in Co-Benefit  
597 Energy scenario compared to the Nationally Determined Contribution scenario in 2035  
598 ([Xing et al., 2021](#)). Although it has been reported that excessive acid gas emission  
599 controls may increase the oxidizing capacity of the atmosphere and increase other  
600 pollution, PM<sub>2.5</sub> concentrations have consistently decreased with previous acid gas  
601 control ([Huang et al., 2021](#)). In addition, under the influence of low-carbon policies,  
602 other pollutant emissions will also be controlled. Opportunities and challenges coexist  
603 in the control of acid gas emissions.

604 In contrast to acid gas emissions, NH<sub>3</sub> emissions predominantly come from  
605 agricultural sources. Although the Chinese government has recognized the importance

606 of NH<sub>3</sub> emissions controls in curbing PM<sub>2.5</sub> pollution, NH<sub>3</sub> emissions reductions have  
607 only been proposed recently as a strategic option and no specific nationwide targets  
608 have yet been implemented (CSC, 2018b). The efficient implementation of NH<sub>3</sub>  
609 reduction options is a major challenge because NH<sub>3</sub> emissions are closely related to  
610 food production, and smallholder farming is still the dominant form of agricultural  
611 production in China. The implementation of NH<sub>3</sub> emissions reduction technologies is  
612 subject to investment in technology, knowledge and infrastructure, and most farmers  
613 are unwilling or economically unable to undertake additional expenditures that cannot  
614 generate financial returns (Gu et al., 2011; Wu et al., 2018b). Therefore, economically  
615 feasible options for NH<sub>3</sub> emission controls need to be developed and implemented  
616 nationwide.

617 We propose the following three requirements that need to be met to achieve  
618 effective reductions of SIA concentrations and hence of PM<sub>2.5</sub> concentrations in China.

619 First, binding targets to reduce both NH<sub>3</sub> and acid gas emissions should be set. The  
620 targets should be designed to meet the PM<sub>2.5</sub> standard, and NH<sub>3</sub> concentrations should  
621 be incorporated into the monitoring system as a government assessment indicator. In  
622 this study, we find large differences in PM<sub>2.5</sub> concentration reductions from NH<sub>3</sub>  
623 emissions reduction in the four megacity regions investigated. At a local scale (i.e., city  
624 or county), the limiting factors may vary within a region (Wang et al., 2011). Thus,  
625 local-specific environmental targets should be considered in policy-making.

626 Second, further strengthening of the controls on acid gas emissions are still needed,  
627 especially under the influence of low-carbon policies, to promote emission reductions  
628 and the adjustment of energy structures and conservation. Ultra-low emissions should  
629 be requirements in the whole production process, including point source emissions,  
630 diffuse source emissions, and clean transportation (Xing et al., 2021; Wang et al.,

631 2021a). The assessment of the impact of ultra-low emissions is provided in Table S6.

632 In terms of energy structure, it is a requirement to eliminate outdated production

633 capacity and promote low-carbon new energy generation technologies.

634 Third, a requirement to promote feasible NH<sub>3</sub> reduction options throughout the

635 whole food production chain, for both crop and animal production. Options include the

636 following. 1) Reduction of nitrogen input at source achieved, for example, through

637 balanced fertilization based on crop needs instead of over-fertilization, and promotion

638 of low-protein feed in animal breeding. 2) Mitigation of NH<sub>3</sub> emissions in food

639 production via, for example, improved fertilization techniques (such as enhanced-

640 efficiency fertilizer (urease inhibitor products), fertilizer deep application, fertilization-

641 irrigation technologies (Zhan et al., 2021), and coverage of solid and slurry manure. 3)

642 Encouragement for the recycling of manure back to croplands, and reduction in manure

643 discarding and long-distance transportation of manure fertilizer. Options for NH<sub>3</sub>

644 emissions control are provided in Table S4. Although the focus here has been on

645 methods to mitigate NH<sub>3</sub> emissions, it is of course critical simultaneously to minimize

646 N losses in other chemical forms such as nitrous oxide gas emissions and aqueous

647 nitrate leaching (Shang et al., 2019; Wang et al., 2020b).

#### 648 4. Conclusions

649 The present study developed an integrated assessment framework using meta-

650 analysis of published literature results, analysis of national monitoring data, and

651 chemical transport modelling to provide insight into the effectiveness of SIA precursor

652 emissions controls in mitigating poor PM<sub>2.5</sub> air quality in China. We found that PM<sub>2.5</sub>

653 concentration significantly decreased in 2000-2019 due to acid gas control policies, but

654 PM<sub>2.5</sub> pollution still severe. Compared with other components, this difference was more

655 significant higher (average increase 98%) for secondary inorganic ions (i.e., SO<sub>4</sub><sup>2-</sup>, NO<sub>3</sub><sup>-</sup>,

656 [and  \$\text{NH}\_4^+\$  on hazy days than on-hazy days.](#) This is mainly caused by the persistent SIA  
657 pollution during the same period. [with sulfate concentrations significantly decreased](#)  
658 and no significant changes observed for nitrate and ammonium concentrations. The  
659 reductions of SIA concentrations in January in megacity clusters of eastern China by  
660 additional 50%  $\text{NH}_3$  emission controls decreased from  $25.9 \pm 0.3\%$  in 2010 to  $22.9 \pm$   
661  $0.3\%$  in 2017, and to  $15 \pm 0.2\%$  in the COVID lockdown in 2020 for simulations  
662 representing reduced acid gas emissions to unprecedented levels, but the SIA  
663 concentrations decreased by  $20.8 \pm 0.3\%$  in 2020 compared with that in 2017 under the  
664 same scenario of an additional 50%  $\text{NH}_3$  emissions reduction. In addition, the reduction  
665 of SIA concentration in 2017 was  $13.4 \pm 0.5\%$  greater for 50% acid gas ( $\text{SO}_2$  and  $\text{NO}_x$ )  
666 reductions than for the  $\text{NH}_3$  emissions reduction. These results indicate that acid gas  
667 emissions need to be further controlled concordantly with  $\text{NH}_3$  reductions to substantially  
668 reduce  $\text{PM}_{2.5}$  pollution in China.

669 Overall, this study provides new insight into the responses of SIA concentrations  
670 in China to past air pollution control policies and the potential balance of benefits in  
671 including  $\text{NH}_3$  emissions reductions with acid gas emissions controls to curb SIA  
672 pollution. The outcomes from this study may also help other countries seeking feasible  
673 strategies to mitigate  $\text{PM}_{2.5}$  pollution.

674

### 675 **Data availability**

676 All data in this study are available from the from the corresponding authors (Wen Xu,  
677 wenxu@cau.edu.cn; Shaocai Yu, shaocaiyu@zju.edu.cn) upon request.

678 **Author contributions**

679 W.X., S.Y., and F.Z. designed the study. F.M., Y.Z., W.X., and J.K. performed the  
680 research. F.M., Y.Z., W.X., and J.K. analyzed the data and interpreted the results. Y.Z.

681 conducted the model simulations. L.L. provided satellite-derived surface NH<sub>3</sub>  
682 concentration. F.M., W.X., Y.Z., and M.R.H. wrote the paper, S. R., M.W., K.W., J.K.,  
683 Y.Z., Y.H., P.L., J.W., Z.C., X.L., M.R.H., S.Y. and F.Z. contributed to the discussion  
684 and revision of the paper.

685 **Declaration of Competing Interest**

686 The authors declare that they have no known competing financial interests or personal  
687 relationships that could have appeared to influence the work reported in this paper.

688 **Acknowledgments**

689 This study was supported by the National Key Research and Development Program of  
690 China (2021YFD1700900), China Scholarship Council (No.201913043), the  
691 Department of Science and Technology of China (No. 2016YFC0202702,  
692 2018YFC0213506 and 2018YFC0213503), National Research Program for Key Issues  
693 in Air Pollution Control in China (No. DQGG0107), National Natural Science  
694 Foundation of China (No. 21577126 and 41561144004), and the High-level Team  
695 Project of China Agricultural University. SR's contribution was supported by the  
696 Natural Environment Research Council award number NE/R000131/1 as part of the  
697 SUNRISE program delivering National Capability.

698 **References**

699 An, Z. S., Huang, R. J., Zhang, R.Y., Tie, X. X., Li, G. H., Cao, J. J., Zhou, W. J., Shi,  
700 Z. G ., Han, Y. M ., Gu, Z. L., and Ji, Y. M.: Severe haze in northern China: A  
701 synergy of anthropogenic emissions and atmospheric processes, Proc. Natl. Acad.  
702 Sci. U. S. A., 116, 8657-8666. <https://doi.org/10.1073/pnas.1900125116>, 2019.  
703 Backes, A., Aulinger, A., Bieser, J., Matthias, V., and Quante, M.: Ammonia emissions

704 in Europe, part II: How ammonia emission abatement strategies affect secondary  
705 aerosols, Atmos. Environ., 126, 153-161,  
706 <https://doi.org/10.1016/j.atmosenv.2015.11.039>, 2016.

707 Bai, Z., Winiwarter, W., Klimont, Z., Velthof, G., Misselbrook, T., Zhao, Z., Jin, X.,  
708 Oenema, O., Hu, C., and Ma, L.: Further improvement of air quality in China needs  
709 clear ammonia mitigation target, Environ. Sci. Technol., 53, 10542-10544,  
710 <https://doi.org/10.1021/acs.est.9b04725>, 2019.

711 Benitez-Lopez, A., Alkemade, R., Schipper, A. M., Ingram, D. J., Verweij, P. A.,  
712 Eikelboom, J. A. J., and Huijbregts, M. A. J.: The impact of hunting on tropical  
713 mammal and bird populations, Science, 356, 180-183, <https://doi.org/10.1126/science.aaq1891>, 2017.

715 Bracken, M. B.: Statistical methods for analysis of effects of treatment in overviews of  
716 randomized trials. In: J.C. Sinclair, M.B. Bracken (Eds.) Effective care of the  
717 newborn infant, Oxford University Press, 1992.

718 Chen, Z.Y., Chen, D.L., Wen, W., Zhuang, Y., Kwan, M.P., Chen, B., Zhao, B., Yang,  
719 L., Gao, B.B., Li, R.Y., and Xu, B.: Evaluating the “2+26” regional strategy for air  
720 quality improvement during two air pollution alerts in Beijing: Variations in PM<sub>2.5</sub>  
721 concentrations, source apportionment, and the relative contribution of local  
722 emission and regional transport, Atmos. Chem. Phys., 19, 6879-6891.  
723 <https://doi.org/10.5194/acp-19-6879-2019>, 2019.

724 Cheng, Y.F., Zheng, G.A., Wei, C., Mu, Q., Zheng, B., Wang, Z.B., Gao, M., Zhang, Q.,  
725 He, K.B., Carmichael, G., Poschl, U., and Su, H.: Reactive nitrogen chemistry in  
726 aerosol water as a source of sulfate during haze events in China, Sci. Adv. 2(12).  
727 <https://doi.org/10.1126/sciadv.1601530>, 2016.

728 China Electricity Council.: China Power Industry Annual Development Report 2019,

729 https://www.cec.org.cn/yaowenkuaidi/2019-06-14/191782.html, 2020.

730 CSC (China State Council): The 11th Five-Year plan on energy saving and emissions  
731 reduction, [http://www.gov.cn/zhengce/content/2008-03/28/content\\_4877.htm](http://www.gov.cn/zhengce/content/2008-03/28/content_4877.htm),  
732 2007.

733 CSC (China State Council): The 12th Five-Year plan on energy saving and emissions  
734 reduction. [http://www.gov.cn/zwgk/2011-12/20/content\\_2024895.htm](http://www.gov.cn/zwgk/2011-12/20/content_2024895.htm), 2011.

735 CSC (China State Council): Action Plan on Prevention and Control of Air Pollution,  
736 China State Council, Beijing, China. [http://www.gov.cn/zwgk/2013-09/12/content\\_2486773.htm](http://www.gov.cn/zwgk/2013-09/12/content_2486773.htm), 2013.

738 CSC (China State Council): The 13th Five-Year plan on energy saving and emissions  
739 reduction. [http://www.gov.cn/zhengce/content/2016-12/05/content\\_5143290.htm](http://www.gov.cn/zhengce/content/2016-12/05/content_5143290.htm),  
740 2016.

741 CSC (China State Council): Air quality targets set by the Action Plan have been fully  
742 realized, [http://www.gov.cn/xinwen/2018-02/01/content\\_5262720.htm](http://www.gov.cn/xinwen/2018-02/01/content_5262720.htm), 2018a.

743 CSC (China State Council): Notice of the state council on issuing the three-year action  
744 plan for winning the Blue Sky defense battle.  
745 [http://www.gov.cn/zhengce/content/2018-07/03/content\\_5303158.htm](http://www.gov.cn/zhengce/content/2018-07/03/content_5303158.htm), 2018b.

746 Dunn, O.J.: Multiple comparisons using rank sums. *Technometrics*, 6, 241-252, 1964.

747 Fountoukis, C., Racherla, P. N., Denier van der Gon, H. A. C., Polymeneas, P.,  
748 Charalampidis, P. E., Pilinis, C., Wiedensohler, A., Dall'Osto, M., O'Dowd, C., and  
749 Pandis, S. N.: Evaluation of a three-dimensional chemical transport model  
750 (PMCAMx) in the European domain during the EUCAARI May 2008 campaign,  
751 *Atmos. Chem. Phys.*, 11, 10331–10347. <https://doi.org/10.5194/acp-11-10331-2011>, 2011.

753 Fan, C., Li, Z., Li, Y., Dong, J., van der A, R., and de Leeuw, G.: Variability of NO<sub>2</sub>

754 concentrations over China and effect on air quality derived from satellite and  
755 ground-based observations, *Atmos. Chem. Phys.*, 21, 7723-7748,  
756 <https://doi.org/10.5194/acp-21-7723-2021>, 2021.

757 Gao, M., Carmichael, G. R., Wang, Y., Saide, P. E., Yu, M., Xin, J., Liu, Z., and Wang,  
758 Z.: Modeling study of the 2010 regional haze event in the North China Plain, *Atmos.*  
759 *Chem. Phys.*, 16, 1673–1691, <https://doi.org/10.5194/acp-16-1673-2016>, 2016.

760 Geng, G.N., Xiao, Q.Y., Zheng, Y.X., Tong, D., Zhang, Y.X., Zhang, X.Y., Zhang, Q.,  
761 He, K.B., and Liu, Y.: Impact of China's air pollution prevention and control action  
762 plan on PM<sub>2.5</sub> chemical composition over eastern China, *Sci China Earth Sci.*, 62,  
763 1872-1884, <https://doi.org/10.1007/s11430-018-9353-x>, 2019.

764 Gu, B. J., Zhu, Y. M., Chang, J., Peng, C. H., Liu, D., Min, Y., Luo, W. D., Howarth, R.  
765 W., and Ge, Y.: The role of technology and policy in mitigating regional nitrogen  
766 pollution, *Environ. Res. Lett.*, 6, 1, <https://doi.org/10.1088/1748-9326/6/1/014011>,  
767 2011.

768 Guenther, A. B., Jiang, X., Heald, CL., Sakulyanontvittaya, T., Duhl, T., Emmons, L.  
769 K., and Wang, X.: The Model of Emissions of Gases and Aerosols from Nature  
770 version 2.1 (MEGAN2.1): an extended and updated framework for modeling  
771 biogenic emissions, *Geosci. Model Dev.*, 5, 1471-1492.  
772 <https://doi.org/10.5194/gmd-5-1471-2012>, 2012.

773 Han, Y., Wu, Y. F., Don, H. Y., and Chen, F.: Characteristics of PM<sub>2.5</sub> and its chemical  
774 composition during the Asia-Pacific Economic Cooperation Summit in Beijing-  
775 Tianjin-Hebei Region and surrounding cities, *Environ. Sci. Technol.*, 40, 134-138  
776 (in Chinese with English abstract), 2017.

777 Huang, R. J., Zhang, Y. L., Bozzetti, C., Ho, K. F., Cao, J. J., Han, Y. M., Daellenbach,  
778 K. R., Slowik, J. G., Platt, S. M., Canonaco, F., Zotter, P., Wolf, R., Pieber, S. M.,

779 Bruns, E. A., Crippa, M., Ciarelli, G., Piazzalunga, A., Schwikowski, M.,  
780 Abbaszade, G., Schnelle-Kreis, J., Zimmermann, R., An, Z. S., Szidat, S.,  
781 Baltensperger, U., El Haddad, I., and Prevot, A. S.: High secondary aerosol  
782 contribution to particulate pollution during haze events in China, *Nature*, 514, 218-  
783 222. <https://doi.org/10.1038/nature13774>, 2014.

784 Huang, X., Ding, A.J, Gao, J., Zheng, B., Zhou, D.R., Qi, X. M., Tang, R., Wang, J. P.,  
785 Ren, C. H., Nie, W., Chi, X. G., Xu, Z., Chen, L. D., Li, Y. Y., Che, F., Pang, N. N.,  
786 Wang, H. K., Tong, D., Qin, W., Cheng, W., Liu, W. J., Fu, Q. Y., Liu, B. X., Chai,  
787 F. H., Davis, S. J., Zhang, Q., and He, K. B.: Enhanced secondary pollution offset  
788 reduction of primary emissions during COVID-19 lockdown in China, *Natl. Sci.*  
789 *Rev.*, 8, 137, <https://doi.org/10.1093/nsr/nwaa137>, 2021.

790 Ianniello, A., Spataro, F., Esposito, G., Allegrini, I ., Rantica, E ., Ancora, MP., Hu, M.,  
791 and Zhu, T.: Occurrence of gas phase ammonia in the area of Beijing (China).  
792 *Atmos. Chem. Phys.*, 10, 9487-9503, <https://doi.org/10.5194/acp-10-9487-2010>,  
793 2010.

794 Kang, Y. N., Liu, M. X., Song, Y., Huang, X ., Yao, H ., Cai, X. H., Zhang, H. S., Kang,  
795 L., Liu, X. J., Yan, X. Y., He, H., Zhang, Q., Shao, M., and Zhu, T.: High-resolution  
796 ammonia emissions inventories in China from 1980 to 2012, *Atmos. Chem. Phys.*,  
797 16, 2043-2058, <https://doi.org/10.5194/acp-16-2043-2016>, 2016.

798 Kruskal, W.H. and Wallis, W.A.: Use of ranks in one-criterion variance  
799 analysis. *Journal of the American statistical Association*, 47, 583-621,  
800 <https://doi.org/10.1080/01621459.1952.10483441>, 1952.

801 Kuerban, M., Waili, Y., Fan, F., Liu, Y., Qin, W., Dore, A. J., Dore, A. J., Xu, W., and  
802 Zhang, F. S.: Spatio-temporal patterns of air pollution in China from 2015 to 2018  
803 and implications for health risks, *Environ. Pollut.*, 258, 113659, <https://doi.org/>

804 10.1016/j.envpol.2019.113659, 2020.

805 Li, H. Y., Zhang, Q., Zheng, B., Chen, C. R., Wu, N. N., Guo, H. Y., Zhang, Y. X., Zheng,  
806 Y. X., Li, X., and He, K. B.: Nitrate-driven urban haze pollution during summertime  
807 over the North China Plain, *Atmos. Chem. Phys.*, 18, 5293-5306, <https://doi.org/10.5194/acp-18-5293-2018>, 2018.

808

809 Li, M., Liu, H., Geng, G., Geng, G. N., Hong, C. P., Liu, F., Song, Y., Tong, D., Zheng,  
810 B., Cui, H. Y., Man, H. Y., Zhang, Q., and He, K. B.: Anthropogenic emission  
811 inventories in China: a review, *Natl. Sci. Rev.*, 4, 834-866.  
812 <https://doi.org/10.1093/nsr/nwx150>, 2017.

813 Liang, F. C., Xiao, Q. Y., Huang, K. Y., Yang, X. L., Liu, F. C., Li, J. X., Lu, X. F., Liu,  
814 Y., and Gu, D. F.: The 17-y spatiotemporal trend of PM<sub>2.5</sub> and its mortality burden  
815 in China, *Proc. Natl. Acad. Sci. U. S. A.*, 117, 25601-25608, <https://doi.org/10.1073/pnas.1919641117>, 2020.

816

817 Liu, J., Han, Y. Q., Tang, X., Zhu, J., and Zhu, T.: Estimating adult mortality attributable  
818 to PM<sub>2.5</sub> exposure in China with assimilated PM<sub>2.5</sub> concentrations based on a ground  
819 monitoring network, *Sci. Total. Environ.*, 568, 1253-1262, <https://doi.org/10.1016/j.scitotenv.2016.05.165>, 2016.

819

820

821 Liu, L., Zhang, X. Y., Wong, A. Y. H., Xu, W., Liu, X. J., Li, Y., Mi, H., Lu, X. H., Zhao,  
822 L. M., Wang, Z., Wu, X. D., and Wei, J.: Estimating global surface ammonia  
823 concentrations inferred from satellite retrievals, *Atmos. Chem. Phys.*, 19, 12051-  
824 12066. <https://doi.org/10.5194/acp-19-12051-2019>, 2019a.

825

826 Liu, M. X., Huang, X., Song, Y., Tang, J., Cao, J. J., Zhang, X. Y., Zhang, Q., Wang, S.  
827 X., Xu, T. T., Kang, L., Cai, X. H., Zhang, H. S., Yang, F. M., Wang, H. B., Yu, J.  
828 Z., Lau, A. K. H., He, L. Y., Huang, X. F., Duan, L., Ding, A. J., Xue, L. K., Gao,  
J., Liu, B., and Zhu, T.: Ammonia emission control in China would mitigate haze

829 pollution and nitrogen deposition, but worsen acid rain, Proc. Natl. Acad. Sci. U. S.  
830 A., 116, 7760-7765, <https://doi.org/10.1073/pnas.1814880116>, 2019b.

831 Liu, X.J., Sha, Z.P., Song, Y., Dong, H.M., Pan, Y.P., Gao, Z.L., Li, Y.E., Ma, L., Dong,  
832 W.X., Hu, C.S., Wang, W.L., Wang, Y., Geng, H., Zheng, Y.H., and Gu, M.N.:  
833 China's atmospheric ammonia emission characteristics, mitigation options and  
834 policy recommendations, Res. Environ. Sci., 34, 149-157,  
835 <https://10.13198/j.issn.1001-6929.2020.11.12>, 2021.

836 Mao, S. S., Chen, T, Fu, J. M., Liang, J. L., An, X. X., Luo, X. X., Zhang, D. W., and  
837 Liu, B. X.: Characteristic analysis for the thick winter air pollution accidents in  
838 Beijing based on the online observations, Journal of Safety and Environment. 1,  
839 1009-6094 ( in Chinese with English abstract), 2018.

840 MEEP. The Ministry of Ecology and Environment of the People's Republic of China,  
841 China Ecological Environment Bulletin.  
842 <http://www.mee.gov.cn/hjzl/sthjzk/zghjzkbg/>, 2019.

843 Megaritis, A., Fountoukis, C., Charalampidis, P. E., Pilinis, C., and Pandis, S. N.:  
844 Response of fine particulate matter concentrations to changes of emissions and  
845 temperature in Europe, Atmos. Chem. Phys., 13, 3423-3443,  
846 <https://doi.org/10.5194/acp-13-3423-2013>, 2013.

847 MEPC. Ministry of Environment Protection of China, Ambient air quality standards  
848 (GB3095–2012). <http://www.mep.gov.cn/>, 2012.

849 Morrison, H., Thompson, G., and Tatarki, V.: Impact of cloud microphysics on the  
850 development of trailing stratiform precipitation in a simulated squall line:  
851 comparison of one- and two-moment schemes, Mon. Weather. Rev., 137, 991-1007.  
852 <https://doi.org/10.1175/2008MWR2556.1>, 2012 .

853 Nakagawa, S. and Santos, E. S. A.: Methodological issues and advances in biological  
854 meta-analysis, *Evol. Ecol.*, 26, 1253-1274. <https://doi.org/10.1007/s10682-012-9555-5>, 2012.

856 Ortiz-Montalvo, D. Häkkinen, S. A. K., Schwier, A. N., Lim, Y. B., Faye McNeill, V.,  
857 and Turpin, B. J.: Ammonium addition (and aerosol pH) has a dramatic impact on  
858 the volatility and yield of glyoxal secondary organic aerosol, *Environ. Sci. Technol.*,  
859 48, 255-262, <https://doi.org/10.1021/es4035667>, 2014.

860 Pinder, R. W., Adams, P. J., and Pandis, S. N.: Ammonia emission controls as a cost-  
861 effective strategy for reducing atmospheric particulate matter in the eastern United  
862 States, *Environ. Sci. Technol.*, 41, 380-386, <https://doi.org/10.1021/es060379a>,  
863 2007.

864 Röllin, H.B., Mathee, A., Bruce, N., Levin, J., and von Schirnding, Y. E.: Comparison  
865 of indoor air quality in electrified and un-electrified dwellings in rural South African  
866 villages. *Indoor Air*, 14, 208-16. <https://doi.org/10.1111/j.1600-0668.2004.00238.x>,  
867 2004.

868 Ronald, J. V., Mijling, B., Ding, J. Y., Koukouli, M. E., Liu, F., Li, Q., Mao, H. Q., and  
869 Theys, N.: Cleaning up the air: effectiveness of air quality policy for SO<sub>2</sub> and NO<sub>x</sub>  
870 emissions in China, *Atmos. Chem. Phys.*, 17, 1775-1789,  
871 <https://doi.org/10.5194/acp-17-1775-2017>, 2017.

872 Shang, Z.Y., Zhou, F., Smith, P., Saikawa, E., Ciais, P., Chang, J.F., Tian, H.Q., Del  
873 Grosso, S.L., Ito, A., Chen, M.P., Wang, Q.H., Bo, Y., Cui, X.Q., Castaldi, S.,  
874 Juszczak, P., Kasimire, A., Magliulo, V., Medinets, S., Medinets, V., Rees, R. M.,  
875 Wohlfahrt, G., and Sabbatini, S: Weakened growth of cropland-N<sub>2</sub>O emissions in  
876 China accociated with nationwide policy interventions, *Glob. Change. Biol.*, 25,  
877 3706-3719, <https://doi.org/10.1111/gcb.14741>, 2021.

878 Sulaymon, I.D., Zhang, Y., Hopke, P. K., Zhang, Y., Hua, J., and Mei, X.: COVID-19  
879 pandemic in Wuhan: Ambient air quality and the relationships between criteria air  
880 pollutants and meteorological variables before, during, and after lockdown, *Atmos*  
881 *Res.*, 250. <https://doi.org/10.1016/j.atmosres.2020.105362>, 2021.

882 Sun, Y. L., Zhuang, G. S., Tang, A. H., Wang, Y., and An, Z. S.: Chemical characteristics  
883 of PM<sub>2.5</sub> and PM<sub>10</sub> in haze-fog episodes in Beijing, *Environ. Sci. Technol.*, 40, 3148-  
884 3155, <https://doi.org/10.1021/es051533g>, 2006.

885 Tao, J., Gao, J., Zhang, L. M., Wang, H., Qiu, X. H., Zhang, Z. S., Wu, Y. F., Chai, F.  
886 H., and Wang, S. L: Chemical and optical characteristics of atmospheric aerosols in  
887 Beijing during the Asia-Pacific Economic Cooperation China 2014, *Atmos.*  
888 *Environ.*, 144, 8-16, <https://doi.org/10.1016/j.atmosenv.2016.08.067>, 2016.

889 Wang S.: How to promote ultra-low emissions during the 14th Five-Year Plan? China.  
890 Environment. News. [http://epaper.cenews.com.cn/html/2021-04/30/node\\_7.htm](http://epaper.cenews.com.cn/html/2021-04/30/node_7.htm),  
891 2021a.

892 Wang, G. H., Zhang, R. Y., Gomez, M. E., Yang, L. X., Zamora, M. L., Hu, M., Lin, Y.,  
893 Peng, J. F., Guo, S., Meng, J. J., Li, J. J., Cheng, C. L., Hu, T. F., Ren, Y. Q., Wang,  
894 Y. S., Gao, J., Cao, J. J., An, Z. S., Zhou, W. J., Li, G. H., Wang, J. Y., Tian, P. F.,  
895 Marrero-Ortiz, W., Secrest, J., Du, Z. F., Zheng, J., Shang, D. J., Zeng, L. M., Shao,  
896 M., Wang, W. G., Huang, Y., Wang, Y., Zhu, Y. J., Li, Y. X., Hu, J. X., Pan, B., Cai,  
897 L., Cheng, Y. T., Ji, Y. M., Zhang, F., Rosenfeld, D., Liss, P. S., Duce, R. A., Kolb,  
898 C. E., and Molina, M. J.: Persistent sulfate formation from London Fog to Chinese  
899 haze, *Proc. Natl. Acad. Sci. U. S. A.*, 113, 13630-13635, <https://doi.org/10.1073/pnas.1616540113>, 2016.

900 Wang, L., Chen, X., Zhang, Y., Li, M., Li, P., Jiang, L., Xia, Y., Li, Z., Li, J., Wang, L.,  
901 Hou, T., Liu, W., Rosenfeld, D., Zhu, T., Zhang, Y., Chen, J., Wang, S., Huang, Y.,

903 Seinfeld, J. H., and Yu, S.: Switching to electric vehicles can lead to significant  
904 reductions of PM<sub>2.5</sub> and NO<sub>2</sub> across China, *One Earth*, 4, 1037–1048,  
905 <https://doi.org/10.1016/j.oneear.2021.06.008>, 2021b.

906 Wang, L., Yu, S., Li, P., Chen, X., Li, Z., Zhang, Y., Li, M., Mehmood, K., Liu, W., Chai,  
907 T., Zhu, Y., Rosenfeld, D., and Seinfeld, J. H.: Significant wintertime PM<sub>2.5</sub>  
908 mitigation in the Yangtze River Delta, China, from 2016 to 2019: observational  
909 constraints on anthropogenic emission controls, *Atmos. Chem. Phys.*, 2, 14787–  
910 14800, <https://doi.org/10.5194/acp-20-14787-2020>, 2020a.

911 Wang, Q.H., Zhou, F., Shang, Z.Y., Ciais, P., Winiwarter, W., Jackson, R. B., Tubiello,  
912 F.N., Janssens-Maenhout, G., Tian, H. Q., Cui, X. Q., Canadell, J.G., Piao, S. L.,  
913 and Tao, S.: Data-driven estimates of global nitrous oxide emissions from cropland,  
914 *Natl. Sci. Rev.*, 7, 441–452, <https://doi.org/10.1093/nsr/nwz087>, 2020b.

915 Wang, S. X., Xing, J., Jang, C., Jang, C. R., Zhu, Y., Fu, J. S., and Hao, J. M.: Impact  
916 assessment of ammonia emissions on inorganic aerosols in East China using  
917 response surface modeling technique, *Environ. Sci. Technol.*, 45, 9293–9300,  
918 <https://doi.org/10.1021/es2022347>, 2011.

919 Wang, Y. H., Wang, Y. S., Wang, L.L., Petaja, T., Zha, Q.Z., Gong, C.S., Li, S.X., Pan,  
920 Y. P., Hu, B., Xin, J. Y., and Kulmala, M.: Increased inorganic aerosol fraction  
921 contributes to air pollution and haze in China, *Atmos. Chem. Phys.*, 19, 5881–5888.  
922 <https://doi.org/10.5194/acp-19-5881-2019>, 2019a.

923 Wang, Y., Zhang, Q. Q., He, K.B., Zhang, Q., and Chai, L.: Sulfate-nitrate-ammonium  
924 aerosols over China: Response to 2000–2015 emission changes of sulfur dioxide,  
925 nitrogen oxides, and ammonia, *Atmos. Chem. Phys.*, 13, 2635–2652.  
926 <https://doi.org/10.5194/acp-13-2635-2013>, 2013.

927 Wang, Y.C., Chen, J., Wang, Q.Y., Qin, Q.D., Ye, J.H., Han, Y.M., Li, L., Zhen, W., Zhi,

928 Q., Zhang, Y.X., and Cao, J.J.: Increased secondary aerosol contribution and  
929 possible processing on polluted winter days in China, *Environ. Int.*, 127.  
930 <https://doi.org/10.1016/j.envint.2019.03.021>, 2019b.

931 Wei, J., Li, Z. Q., Cribb, M., Huang, W., Xue, W.H., Sun, L., Guo, J. P., Peng, Y. R., Li,  
932 J., and Lyapustin, A.: Improved 1 km resolution PM<sub>2.5</sub> estimates across China using  
933 enhanced space–time extremely randomized trees, *Atmos. Chem. Phys.*, 20, 3273–  
934 3289. <https://doi.org/10.5194/acp-20-3273-2020>, 2020.

935 Wei, J., Li, Z. Q., Lyapustin, A., Sun, L., Peng, Y. R., Xue, W. H., Su, T. N., and Cribb,  
936 M.: Reconstructing 1-km-resolution high-quality PM<sub>2.5</sub> data records from 2000 to  
937 2018 in China: spatiotemporal variations and policy implications, *Remote. Sens.*  
938 *Environ.*, 252, 112136, <https://doi.org/10.1016/j.rse.2020.112136>, 2021.

939 Wu, Y. J., Wang, P., Yu, S. C., Wang, L. Q., Li, P. F., Li, Z., Mehmood, K., Liu, W. P.,  
940 Wu, J., Lichtfouse, E., Rosenfeld, D., and Seinfeld, J. H.: Residential emissions  
941 predicted as a major source of fine particulate matter in winter over the Yangtze  
942 River Delta, China, *Environ. Chem. Lett.*, 16, 1117–1127.  
943 <https://doi.org/10.1007/s10311-018-0735-6>, 2018a.

944 Wu, Y. Y., Xi, X. C., Tang, X., Luo, D. M., Gu, B. J., Lam, S. K., Vitousek, P. M., and  
945 Chen, D. L.: Policy distortions, farm size, and the overuse of agricultural chemicals  
946 in China, *Proc. Natl. Acad. Sci. U. S. A.*, 115, 7010–7015.  
947 <https://doi.org/10.1073/pnas.1806645115>, 2018b.

948 Xiao, Q.Y., Geng, G.N., Liang, F.C., Wang, X., Lv, Z., Lei, Y., Huang, X.M., Zhang, Q.,  
949 Liu, Y., and He, K.B: Changes in spatial patterns of PM<sub>2.5</sub> pollution in China 2000–  
950 2018: Impact of clean air policies, *Environ. Int.*, 141, 105776, <https://doi.org/10.1016/j.envint.2020.105776>, 2020.

952 Xiao, Q.Y., Zheng, Y.X., Geng, G.N., Chen, C.H., Huang, X.M., Che, H.Z., Zhang, X.Y.,

953 He, K.B., and Zhang, Q.: Separating emission and meteorological contribution to  
954 PM<sub>2.5</sub> trends over East China during 2000–2018, *Atmos. Chem. Phys.*, 21, 9475-  
955 9496, <https://doi.org/10.5194/acp-21-9475-2021>, 2021.

956 Xing, J., Liu, X., Wang, S. X., Wang, T., Ding, D., Yu, S., Shindell, D., Ou, Y .,  
957 Morawska, L., Li, S. W., Ren, L., Zhang, Y. Q., Loughlin, D., Zheng, H. T., Zhao,  
958 B., Liu, S. C., Smith, K. R., and Hao, J. M.: The quest for improved air quality may  
959 push China to continue its CO<sub>2</sub> reduction beyond the Paris Commitment, *Proc. Natl.*  
960 *Acad. Sci. U. S. A.*, 117, 29535-29542, <https://doi.org/10.1073/pnas.2013297117>,  
961 2021.

962 Xu, Q. C., Wang, S. X., Jiang, J. K., Bhattarai, N., Li, X. X., Chang, X., Qiu, X. H.,  
963 Zheng, M., Hua, Y., and Hao, J. M.: Nitrate dominates the chemical composition of  
964 PM<sub>2.5</sub> during haze event in Beijing, China, *Sci. Total. Environ.*, 689, 1293-1303,  
965 <https://doi.org/10.1016/j.scitotenv.2019.06.294>, 2019.

966 Xu, W., Song, W., Zhang, Y. Y., Liu, X. J., Zhang, L., Zhao, Y. H., Liu, D. Y., Tang, A.  
967 H., Yang, D. W., Wang, D. D., Wen, Z., Pan, Y. P., Fowler, D., Collett, J. L., Erisman,  
968 J. W., Goulding, K., Li, Y., and Zhang, F. S.: Air quality improvement in a megacity:  
969 implications from 2015 Beijing Parade Blue pollution control actions, *Atmos.*  
970 *Chem. Phys.*, 17, 31-46. <https://doi.org/10.5194/acp-17-31-2017>, 2017.

971 Xu, W., Wu, Q.H., Liu, X.J., Tang, A.H., Dore, A.J., and Heal, M.R.: Characteristics of  
972 ammonia, acid gases, and PM<sub>2.5</sub> for three typical land-use types in the North China  
973 Plain, *Environ Sci Pollut R.*, 23, 1158-1172. [https://doi.org/10.1007/s11356-015-5648-3](https://doi.org/10.1007/s11356-015-<br/>974 5648-3), 2016.

975 Xue, T., Liu, J., Zhang, Q., Geng, G.N., Zheng, Y.X., Tong, D., Liu, Z., Guan, D.B., Bo,  
976 Y., Zhu, T., He, K.B., and Hao, J.M.: Rapid improvement of PM<sub>2.5</sub> pollution and  
977 associated health benefits in China during 2013–2017, *Sci. China Earth Sci.*, 62,

978 1847-1856, <https://doi.org/10.1007/s11430-018-9348-2>, 2019.

979 Yang, F., Tan, J., Zhao, Q., Du, Z., He, K., Ma, Y., Duan, F., Chen, G., and Zhao, Q.:  
980 Characteristics of PM<sub>2.5</sub> speciation in representative megacities and across China.  
981 *Atmos. Chem. Phys.*, 11, 5207-5219, <https://doi.org/10.5194/acp-11-5207-2011>,  
982 2011.

983 Ying, H., Yin, Y. L., Zheng, H. F., Wang, Y. C., Zhang, Q. S., Xue, Y. F., Stefanovski,  
984 D., Cui, Z. L., and Dou, Z. X.: Newer and select maize, wheat, and rice varieties  
985 can help mitigate N footprint while producing more grain, *Glob. Change. Biol.*, 12,  
986 4273-4281, <https://doi.org/10.1111/gcb.14798>, 2019.

987 Yu, S.C., Dennis, R., Roselle, S., Nenes, A., Walker, J., Eder, B., Schere, K., Swall, J.,  
988 and Robarge, W.: An assessment of the ability of three-dimensional air quality  
989 models with current thermodynamic equilibrium models to predict aerosol NO<sub>3</sub><sup>-</sup>, *J  
990 Geophys Res-Atmos.*, 110(D7). <https://doi.org/10.1029/2004JD004718>, 2005.

991 Yue, H. B., He, C. Y., Huang, Q. X., Yin, D., and Bryan, B. A.: Stronger policy required  
992 to substantially reduce deaths from PM<sub>2.5</sub> pollution in China, *Nat. Commun.*, 11,  
993 1462, <https://doi.org/10.1038/s41467-020-15319-4>, 2020.

994 Zhan, X.Y., Adalibieke, W., Cui, X.Q., Winiwarter, W., Reis, S., Zhang, L., Bai, Z.H.,  
995 Wang, Q.H., Huang, W.C., and Zhou, F.: Improved estimates of ammonia emissions  
996 from global croplands, *Environ. Sci. Technol.*, 55, 1329-1338,  
997 <https://doi.org/10.1021/acs.est.0c05149>, 2021.

998 Zhang, L., Jacob, D. J., Knipping, E. M., Kumar, N., Munger, J. W., Carouge, C. C.,  
999 van Donkelaar, A., Wang, Y. X., and Chen, D: Nitrogen deposition to the United  
1000 States: distribution, sources, and processes, *Atmos. Chem. Phys.*, 12, 4539–4554,  
1001 <https://doi.org/10.5194/acp-12-4539-2012>, 2012.

1002 Zhang, Q., Zheng, Y. X., Tong, D., Shao, M., Wang, S. X., Zhang, Y. H., Xu, X. D.,

1003 Wang, J. N., He, H., Liu, W. Q., Ding, Y. H., Lei, Y., Li, J. H., Wang, Z. F., Zhang,  
1004 X. Y., Wang, Y. S., Cheng, J., Liu, Y., Shi, Q. R., Yan, L., Geng, G. N., Hong, C. P.,  
1005 Li, M., Liu, F., Zheng, B., Cao, J. J., Ding, A. J., Gao, J., Fu, Q. Y., Huo, J. T., Liu,  
1006 B. X., Liu, Z. R., Yang, F. M., He, K. B., and Hao, J. M.: Drivers of improved PM<sub>2.5</sub>  
1007 air quality in China from 2013 to 2017, Proc. Natl. Acad. Sci. U. S. A., 49, 24463-  
1008 24469, <https://doi.org/10.1073/pnas.1907956116>, 2019.

1009 Zhang, X. M., Gu, B. J., van Grinsven, H., Lam, S.K., Liang, X., Bai, M., and Chen,  
1010 D.L.: Societal benefits of halving agricultural ammonia emissions in China far  
1011 exceed the abatement costs. Nat. Commun., 11, 4357,  
1012 <https://doi.org/10.1038/s41467-020-18196-z>, 2020.

1013 Zhang, Y., Chen, X., Yu, S., Wang, L., Li, Z., Li, M., Liu, W., Li, P., Rosenfeld, D., and  
1014 Seinfeld, J. H: City-level air quality improvement in the Beijing-Tianjin-Hebei  
1015 region from 2016/17 to 2017/18 heating seasons: Attributions and process analysis,  
1016 Environ. Pollut., 274, <https://doi.org/10.1016/j.envpol.2021.116523>, 2021a.

1017 Zhang, Y.Y., Liu, X.J., Zhang, L., Tang, A.H., Goulding, K., and Collett Jr, J.L.:  
1018 Evolution of secondary inorganic aerosols amidst improving PM<sub>2.5</sub> air quality in  
1019 the North China Plain, Environ. Pollut., 281, 117027,  
1020 <https://doi.org/10.1016/j.envpol.2021.117027>, 2021b.

1021 Zheng, B., Tong, D., Li, M., Hong, C. P., Geng, G. N., Li, H. Y., Li, X., Peng, L. Q.,  
1022 Qi, J., Yan, L., Zhang, Y. X., Zhao, H. Y., Zheng, Y. X., He, K. B., and Zhang, Q.:  
1023 Trends in China's anthropogenic emissions since 2010 as the consequence of clean  
1024 air actions, Atmos. Chem. Phys., 18, 14095-14111, <https://doi.org/10.5194/acp-18-14095-2018>, 2018.

1025  
1026  
1027